UNIVERSITY OF CALIFORNIA
RIVERSIDE

Microbiome in the Middle: Examining the Lung Microbiome as an Interface Between Host and Environment

A Dissertation submitted in partial satisfaction
of the requirements for the degree of

Doctor of Philosophy

in

Microbiology

by

Talyssa Monje Topacio

September 2025

Dissertation Committee:
Dr. Emma Aronson, Chairperson
Dr. Ansel Hsiao
Dr. David Lo

The Dissertation of Talyssa Monje Topacio is approved:

_____

_____

_____

Committee Chairperson

University of California, Riverside

Acknowledgements

Thank you to my advisor, Dr. Emma Aronson, for offering me the opportunity to take part in this major interdisciplinary project. I've learned so much and it's no doubt that I've grown immensely as a scientist thanks to your trust and confidence in me to explore these big questions. I think we have both managed to learn so much as this project came to fruition, so thank you for your shared enthusiasm and continuous support.

To my committee, Dr. David Lo and Dr. Ansel Hsiao; thank you both for your ongoing support through every evolution of this project. Dr. David Lo, thank you for giving me the space to learn almost everything I know about host immunology and for your active collaboration on this research. This project would quite literally not have been possible without you and your lab's support. Dr. Ansel Hsiao, thank you for offering a voice of reason during some of my most confused moments. It's easy to get lost in the weeds of big data, so I greatly appreciate the grounding reminders.

To Dr. Mia Maltz, thank you for trusting me to build upon your foundations of this project and for your ongoing collaboration. I truly appreciate how much you've supported me through this research, analysis, and writing and I'm so grateful we have gotten to work together all this time.

To my lab mate, Dr. Linton Freund—we've done it! I am eternally grateful for your support through our entire tenure. I can't even fathom what it might've been like to experience the highs and lows of grad school without your presence and knowledge, so I truly thank you for everything!

To Marina Zaza, what would I have done without you?! Thank you for working so

hard on the long chamber exhaust days and stepping up as a leader in the lab to help me out as my workload became a seemingly impossible feat. I'm so grateful for your willingness to support me, your enthusiasm to learn new things, and of course, for all your entertaining stories. You are an amazing and knowledgeable scientist, and you will always have my support!

To all the past and present Aronson Lab members, Dr. Mia Maltz, Dr. Linton Freund, Marina Zaza, Abbey Lyew, Dr. Jerald Ibal, Jordan Dagan, Robin Bond, thank you all for supporting all the aspects of this project. Abbey, thank you for your willingness to step up and take the lead on so many new iterations of this research. You're an absolute joy to work with, and I can't wait to see how your project evolves. Jordan and Robin, thank you both for your respective time spent managing the lab and doing the tedious tasks that ensure everything else runs smoothly. It has been a pleasure to work with you both. Dr. Jerald Ibal, thank you for your recent support and ideas on the analysis for this project, it's so valuable to have received feedback from new perspectives. Thank you to Linton Freund, Robin Bond, Mark Swenson, Jorge Pastrana, and the countless undergraduates and volunteers for the field work and dust collection processing you've done. This work would not have been possible without your time and effort!

This project has been made possible with the help and feedback of so many collaborators. A massive thank you to the Lo lab; Dr. Keziyah Yisrael-Gayle, Dr. Trevor Biddle, Diana Del Castillo, Troy Alaama, Malia Shapiro, and Veronica Penuelas. You have all dedicated so much time to teach me everything I know on the host-immunology side of this project; I have no idea how I would've figured it out without the support from

every single one of you. I'd especially like to give my endless gratitude for the first chamber exposure experiments I had to lead on my own—I genuinely have no clue how those would've played out without you guys' helping hands. To the Cocker lab engineers, Hovanness Dingilian, Dr. Ryan Drover, and Danny Gonzalez, you've all been so integral to your respective chamber exposure runs, thank you for helping to keep these experiments afloat and offering so much of your time and knowledge to make them happen, it has been a pleasure to work with you all.

I would like to extend my thanks to all the scientists and educators that have motivated my passion for biology and will forever be my inspiration. Thank you to Ms. Faith Fitzgerald, my AP biology teacher, for opening me up to the possibility of going off to college to study science. Thank you to Dr. Nancy Fujishige, who led me through my very first research projects at LMU and offered me all the support I needed to matriculate into a graduate program. Thank you to Dr. Martina Ramirez, who offered me invaluable guidance and peace of mind. Thank you to Tanya Kuzmenko, Dr. Michelle Lum, and Dr. Demian Willette for setting exceptional examples as educators that I continue to admire to this day. To Beth Marsh, thank you for providing the space and resources that made it possible for me and my peers in McNair to pursue graduate school with confidence.

I would have never been able to persist without the support of my loved ones who have not only celebrated my epic highs but stuck with me through the epic lows—I'm so happy to be able to share this with you all. To Noeva and Tatum, my mom and sister, I will always be grateful for having a family that shows up for me in the ways I need it the most, thank you both being my lifeline and providing me with unconditional support. In

remembrance of Louis, my dead dad, who has inevitably contributed to so many aspects of this journey. To Boson (I wish she could read this), my baby cat and needy roommate, thank you for being my joy and comfort, I can't imagine having done this without you. To Coco, Kristina, Zoe, my best friends in every universe, thank you for always being there to GAFATIOWNOEGAF. You guys have seen it all and are stuck with me forever— yay! To Felix, Dakfu and Gina, thank you for bringing me outside (literally and figuratively), and for you guys' endless trust and generosity… btw, I am once again available to play Fortnite. To Derek, thank you for helping me stay afloat in this home stretch, your support has meant the world to me and I'm so grateful.

To my Close Friends, thank you for being here to witness the journey. To Dr. Jericho Ortañez, thank you for shouting me out in your acknowledgements. Of course, thank you to my extended family and friends who are always there to celebrate.

Finally, I'd like to acknowledge that all the support, opportunities, and circumstances that have guided me to the end of my PhD have been an absolute privilege, and that the system is not too generous to those who can't conform to it. To my peers beyond academia with an unwavering curiosity and passion for learning more about the world around them, thank you for reminding me why I'm here in the first place. That's what science is about.

Dedicated to everyone I am

ABSTRACT OF THE DISSERTATION

Microbiome in the Middle: Examining the Lung Microbiome as an Interface Between Host and Environment

by

Talyssa Monje Topacio

Doctor of Philosophy, Graduate Program in Microbiology
University of California, Riverside, September 2025
Dr. Emma Aronson, Chairperson

During normal respiration, foreign materials are routinely introduced into the mammalian airway, but host defense mechanisms such as coughing, mucosal clearance, and biochemical regulation typically prevent these materials from reaching the lower respiratory tract (LRT). Historically, the effectiveness of these defenses supported the belief that the respiratory tract was sterile. However, research within the past two decades has revealed a “steady-state, low-level” microbiome of the LRT that develops in parallel to the host immune system and aids in pathogen defense and immune cell recruitment. While existing studies have characterized the relationship between environmental dust and pulmonary health, research examining how air quality influences lung microbiome assembly is limited. Here, we exposed mice to environmental dust samples collected from Southern California’s Salton Sea basin to simulate chronic exposures and observe their effects on host health and the lung microbiome. We used flow cytometry to examine pulmonary inflammation, and 16S rRNA (V3-V4) targeted amplicon sequencing to characterize lung microbiome composition and diversity after dust exposure. We found that overall shifts in lung microbiome diversity and composition after exposure were not directly correlated with the magnitude of neutrophilic pulmonary inflammation, and that

spatiotemporal variation in dust differentially affected lung microbiome composition. We also revealed that increases in lung microbiome diversity and richness were inversely correlated to that of the fecal microbiome, suggesting a systemic stress response to inflammatory environmental dusts. Further, we observed the dispersion of viable bacterial cells in lung tissues following intranasal exposure and visualized preferential maintenance of lung microbiome dynamics through microbial clearance. Our findings suggest that the lung microbiome is responsive to variable characteristics of environmental aerosols, and demonstrate a relationship between environmental dusts, host health, and the lung microbiome. With air pollution becoming a growing concern among rural and urban communities, understanding how we interact with and respond to our environment will come to shape public health strategies. Elucidating this relationship between respiratory health and the lung microbiome opens an opportunity for potential interventions.

Table of Contents

List of Figures

Introduction

The Lung Microbiome

The human microbiome refers to the trillions of symbiotic bacteria, fungi, and viruses associated with the human body. Major clinical and lab-based studies have been able to characterize the distinct microbiome compositions at different body sites and define their roles in host metabolism, disease mediation, and protection against pathogens among many other functions (1,2). Particularly in the lung—which had once been considered sterile— the advancement of molecular techniques within the last two decades have revealed that the lung harbors its own low-level steady-state microbiome which begins to develop immediately after birth, in parallel to the immune system (3). Despite the immunological and mechanical clearance mechanisms in place to eliminate pathogen immigration into the lower respiratory tract, microbiota of the genera *Streptococcus*, *Prevotella*, *Veillonella*, *Fusobacterium*, and *Haemophilus* have been consistently detected in the lungs of healthy human subjects (4,5). In the instance of pulmonary disease, studies have speculated that "disruption" to the lung microbiome can be observed, with genera like *Pseudomonas* being represented at higher relative abundances in patients of asthma and chronic obstructive pulmonary disease. However, overall variation in lung microbiome diversity and taxa relative abundances vary among disease phenotypes, and microbiome dynamics leading up to specific taxa enrichment have yet to be understood (3,6,7).

Lung microbiome function is also less understood. Its parallel development with the neonatal immune system has implied its role in immune regulation within the

pulmonary tract, but its systemic influence beyond the lung is superficially known. The "gut-lung axis", for example, has been hypothesized to be the route of metabolic crosstalk between the gut and lung microbiomes. Due to the gut microbiome's significant role in immune system modulation and regulation through short chain fatty acid (SCFA) and cytokine production, it is believed that systemic recognition of these commensal microbial byproducts aid in proper immune function in the lung. Further, it is speculated that direct migration of immune cells produced in the gut to the lung via circulation can occur to reinforce host defenses against infection or mediate inflammation (8–11). Conversely, the gut microbiome is responsive to systemic stressors such as antibiotic treatment, dietary deficits, infection, and disease. In such instances, gut microbiome composition and diversity has been found to change significantly. Thus, microbiome modulation along the gut-lung axis might also be observed in the opposite "lung-gut" direction in the case of severe pulmonary disease and inflammation (12).

Given this research, it is necessary to consider the role of the lung microbiome at the interface of internal host health and one's external environment. Unlike the gut, the lung is consistently receiving direct input from the environment by way of normal breathing. Although the topography of the lung microbiome is highly contingent on microbial migration from the oropharynx by way of microaspiration, and subsequent clearance via mucociliary action (5,13), the lung's physical vulnerability to environmental triggers may present an additional hurdle for the lung microbiome to overcome.

Pulmonary Health & The Environment

Air pollution is a growing public health concern in both urban and rural environments as energy demands heighten and anthropogenic activity continues to disturb the environment. Particulate matter (PM) deposition in the airway has been attributed to adverse health consequences with fine $PM_{2.5}$ being estimated as the cause of 3.3 million deaths per year worldwide (14). Further, environmental triggers have been suspected to contribute to increased respiratory disease morbidity and exacerbation. Epidemiological studies have shown that chronic exposure to elevated air pollution levels is associated with chronic bronchitis and lung function impairment and leads to overall increases in hospital-related visits for short term exacerbations in chronic obstructive pulmonary disease (COPD) and asthma patients (15). Similarly, air pollution was found to be significantly problematic for child pulmonary function with increased exposure in an urban city being associated with decreased lung function (16).

Climate change is exacerbating major dust storm events. Although windblown dust is ubiquitous in the atmosphere, its ability to be transported across long distances demonstrates its capacity to affect communities within a broad, sometimes transcontinental, range (17–19). While atmospheric dust events have been shown to elicit adverse pulmonary health effects among various regions (20), predominantly low-income, nonwhite communities situated in closer proximity to high-emission environments have been found to be particularly vulnerable to increased outdoor pollution levels and thus, higher incidence of pulmonary disease (21–23). Thus, a combination of socioeconomic and environmental inequity in the context of climate

change is necessary to consider when examining the consequences of environmental triggers and health outcomes.

Respiratory Health at The Salton Sea

In California's Imperial Valley, the Salton Sea is rapidly desiccating after freshwater diversions have subjected the land-locked lake to increasing temperatures and drought in the arid desert climate (24). Consequently, agricultural runoff has made its way into the lakebed, leading to hypersalinity and nutrient loading which has been fatal for the once rich and diverse marine environment. As Salton Sea marine ecology worsens, regional dust events become a growing concern due to newly exposed, contaminant-laden playa sediment becoming entrained in the air (25–28).

What is already a worsening ecological crisis is also a major public health concern. The Salton Sea region has been ranked as having one of the highest percentages of asthma related hospital visits in the state of California, and regional reports for cases of childhood asthma are disproportionately higher in comparison to the state and national averages (23,29,30). The inflammatory nature of Salton Sea dust exposures in controlled mouse studies (31) have led us to assume a direct correlation between environmental dust composition and local respiratory health; however, a detailed understanding of this relationship will be necessary for ecological intervention and a broader understanding of exposure-related pulmonary inflammation.

The work presented in this dissertation aims to elucidate the relationship between ecological and pulmonary health by assessing the influence of environmental dust

exposures on the lung microbiome. In the first chapter, we determine the effect of dust-induced pulmonary inflammation on lung microbiome diversity and composition. In the second chapter, we examine how spatiotemporal variation of dust differentially affects the lung and fecal microbiomes. Finally, in the third chapter, we compare methods of live bacterial introduction in the lung to assess microbial clearance over time.

References

1. The Human Microbiome Project Consortium. Structure, function and diversity of the healthy human microbiome. Nature. 2012 Jun;486(7402):207–14.

2. Ursell LK, Metcalf JL, Parfrey LW, Knight R. Defining the human microbiome. Nutr Rev. 2012 Aug;70:S38–44.

3. Kostric M, Milger K, Krauss-Etschmann S, Engel M, Vestergaard G, Schloter M, et al. Development of a Stable Lung Microbiome in Healthy Neonatal Mice. Microb Ecol. 2018 Feb;75(2):529–42.

4. Hilty M, Burke C, Pedro H, Cardenas P, Bush A, Bossley C, et al. Disordered Microbial Communities in Asthmatic Airways. Neyrolles O, editor. PLoS ONE. 2010 Jan 5;5(1):e8578.

5. Whiteside SA, McGinniss JE, Collman RG. The lung microbiome: progress and promise. J Clin Invest. 2021 Aug 2;131(15):e150473.

6. Dickson RP, Erb-Downward JR, Huffnagle GB. The role of the bacterial microbiome in lung disease. Expert Rev Respir Med. 2013 Jun;7(3):245–57.

7. Natalini JG, Singh S, Segal LN. The dynamic lung microbiome in health and disease. Nat Rev Microbiol. 2023 Apr;21(4):222–35.

8. Wypych TP, Wickramasinghe LC, Marsland BJ. The influence of the microbiome on respiratory health. Nat Immunol. 2019 Oct;20(10):1279–90.

9. Zhang J, Zheng X, Luo W, Sun B. Cross-domain microbiomes: the interaction of gut, lung and environmental microbiota in asthma pathogenesis. Front Nutr. 2024 Jun 21;11:1346923.

10. Bidell MR, Hobbs ALV, Lodise TP. Gut microbiome health and dysbiosis: A clinical primer. Pharmacother J Hum Pharmacol Drug Ther. 2022 Nov;42(11):849–57.

11. He Y, Wen Q, Yao F, Xu D, Huang Y, Wang J. Gut–lung axis: The microbial contributions and clinical implications. Crit Rev Microbiol. 2017 Jan 2;43(1):81–95.

12. Bowerman KL, Rehman SF, Vaughan A, Lachner N, Budden KF, Kim RY, et al. Disease-associated gut microbiome and metabolome changes in patients with chronic obstructive pulmonary disease. Nat Commun. 2020 Nov 18;11(1):5886.

13. Dickson RP, Erb-Downward JR, Freeman CM, McCloskey L, Falkowski NR, Huffnagle GB, et al. Bacterial Topography of the Healthy Human Lower Respiratory Tract. Clemente JC, editor. mBio. 2017 Mar 8;8(1):e02287-16.

14. Kurt OK, Zhang J, Pinkerton KE. Pulmonary health effects of air pollution: Curr Opin Pulm Med. 2016 Mar;22(2):138–43.

15. Viegi G, Maio S, Pistelli F, Baldacci S, Carrozzi L. Epidemiology of chronic obstructive pulmonary disease: Health effects of air pollution. Respirology. 2006 Sep;11(5):523–32.

16. Tabaku A, Bejtja G, Bala S, Toci E, Resuli J. Effects of air pollution on children's pulmonary health. Atmos Environ. 2011 Dec;45(40):7540–5.

17. Yamaguchi N, Park J, Kodama M, Ichijo T, Baba T, Nasu M. Changes in the Airborne Bacterial Community in Outdoor Environments following Asian Dust Events. Microbes Environ. 2014;29(1):82–8.

18. Rublee CS, Sorensen CJ, Lemery J, Wade TJ, Sams EA, Hilborn ED, et al. Associations Between Dust Storms and Intensive Care Unit Admissions in the United States, 2000–2015. GeoHealth. 2020 Aug;4(8):e2020GH000260.

19. Miao Y, Porter WC, Benmarhnia T, Lowe C, Lyons TW, Hung C, et al. Source-specific acute cardio-respiratory effects of ambient coarse particulate matter exposure in California's Salton Sea region. Environ Res Health. 2025 Mar 1;3(1):015006.

20. Esmaeil N, Gharagozloo M, Rezaei A, Grunig G. Dust events, pulmonary diseases and immune system.

21. Bell ML, O'Neill MS, Cifuentes LA, Braga ALF, Green C, Nweke A, et al. Challenges and recommendations for the study of socioeconomic factors and air pollution health effects. Environ Sci Policy. 2005 Oct;8(5):525–33.

22. Marshall JD. Environmental inequality: Air pollution exposures in California's South Coast Air Basin. Atmos Environ. 2008 Jul;42(21):5499–503.

23. Miao Y, Porter WC, Schwabe K, LeComte-Hinely J. Evaluating health outcome metrics and their connections to air pollution and vulnerability in Southern California's Coachella Valley. Sci Total Environ. 2022 May;821:153255.

24. Johnston JE, Razafy M, Lugo H, Olmedo L, Farzan SF. The disappearing Salton Sea: A critical reflection on the emerging environmental threat of disappearing saline lakes and potential impacts on children's health. Sci Total Environ. 2019 May;663:804–17.

25. Hung C, Diamond C, Sinclair R, Lee MC, Stenstrom M, Freilich MA, et al. Nutrient loading as a key cause of short- and long-term anthropogenic ecological degradation of the Salton Sea. Sci Rep. 2024 Dec 28;14(1):31247.

26. Jones BA, Fleck J. Shrinking lakes, air pollution, and human health: Evidence from California's Salton Sea. Sci Total Environ. 2020 Apr;712:136490.

27. Reese BK, Anderson MA, Amrhein C. Hydrogen sulfide production and volatilization in a polymictic eutrophic saline lake, Salton Sea, California. Sci Total Environ. 2008 Nov;406(1–2):205–18.

28. Frie AL, Dingle JH, Ying SC, Bahreini R. The Effect of a Receding Saline Lake (The Salton Sea) on Airborne Particulate Matter Composition. Environ Sci Technol. 2017 Aug 1;51(15):8283–92.

29. Marshall J. Why Emergency Physicians Should Care About the Salton Sea. West J Emerg Med. 2017 Oct 18;18(6):1008–9.

30. Farzan SF, Razafy M, Eckel SP, Olmedo L, Bejarano E, Johnston JE. Assessment of Respiratory Health Symptoms and Asthma in Children near a Drying Saline Lake. Int J Environ Res Public Health. 2019 Oct 11;16(20):3828.

31. Biddle TA, Yisrael K, Drover R, Li Q, Maltz MR, Topacio TM, et al. Aerosolized aqueous dust extracts collected near a drying lake trigger acute neutrophilic pulmonary inflammation reminiscent of microbial innate immune ligands. Sci Total Environ. 2023 Feb;858:159882.

CHAPTER I

Title: Lung microbiomes' variable responses to dust exposure

Authors: Mia R. Maltz[1*+], Talyssa M. Topacio[2*], David D. Lo[3], Marina Zaza[2], Linton Freund[4], Jon Botthoff[5], Mark Swenson[2], David Cocker[6], Trevor Biddle[3], Keziyah Yisrael[3], Diana del Castillo[3], Ryan Drover[6], Emma Aronson[2,5]

[1] University of Connecticut, Department of Plant Sciences and Landscape Architecture, Storrs, CT

[2] University of California, Riverside. Department of Microbiology and Plant Pathology, Riverside, CA

[3] University of California, Riverside. Department of Biomedical Sciences, Riverside, CA

[4] University of California, San Diego. Department of Medicine, San Diego, CA

[5] University of California, Riverside. Center for Conservation Biology, Riverside, CA

[6] University of California, Riverside. Department of Chemical Environmental Engineering, Riverside, CA

*These indicate co-first authors that contributed equally towards experimental manipulations and manuscript preparation.

Abstract

Inhalation of dust is significant and relevant to health effects. As pollution and climate change worsen in dryland regions, wind currents entrain loose sediment and dust. This potentially disperses toxic geochemical and microbial burdens throughout the region. When inhaled environmental dust and host-associated microbiomes mingle, they pose exposure risks to host respiratory health. The Salton Sea, California's largest lake, is shrinking thus exposing nearby communities to playa dust. Therefore, we analyze the effect of Salton Sea dust exposure in murine models to relate lung microbial communities and respiratory health. We used an environmental chamber to expose mice to dust filtrate or ambient air and examined the effects of those exposures on lung microbiomes. We found that lung microbial composition varied by dust exposure. Furthermore, dust elicited neutrophil recruitment and immune responses more than mice exposed to ambient air. Sources of dust differentially affected the composition of the lung core microbiome. Lung microbial diversity correlated with neutrophil recruitment as lungs associated with inflammatory responses harbored more diverse microbiomes. Although Salton Sea dust influences dust microbiomes and prevalent taxa, these responses were variable. The composition of lungs exposed to dust collected further from the Sea was more similar to lungs from ambient air exposures; in contrast, dust collected near the Sea yielded lung microbiomes that clustered further from lungs exposed to ambient air. As lakes continue to dry out, we expect greater public health risks in proximal dryland regions, which may correlate with dust microbial dispersal-related changes to lung microbiomes

Graphical Abstract

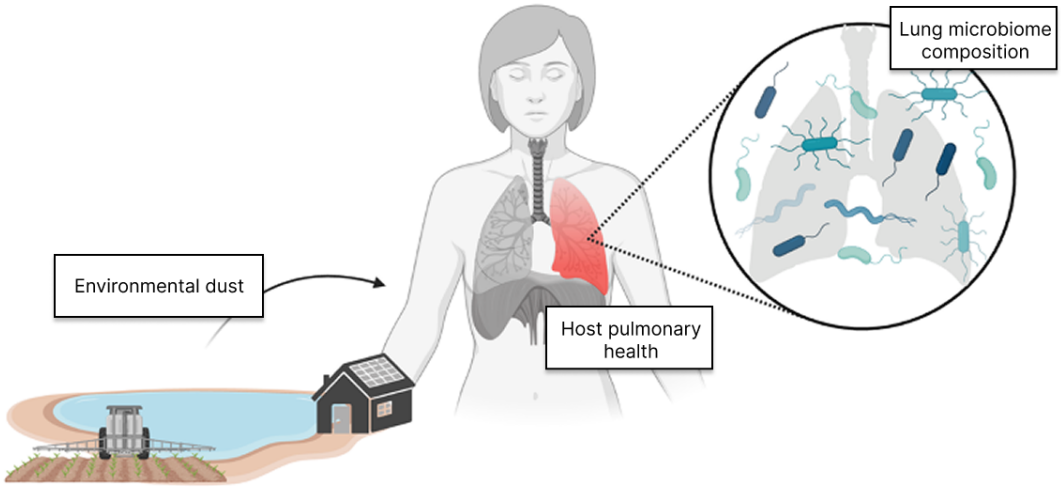

Introduction

Major dust storms originating in natural desert regions like the Sahara, Australian, and Gobi deserts can carry particulate matter across oceans and continents (1,2). Local dust events that occur in dryland environments and near human settlements are of mounting concern for humans and wildlife. The aeolian environment harbors a variety of airborne particulates composed of both geological and biochemical components, reflective of their provenance (3). At saline terminal lakes, water resource diversion and rising temperatures that exacerbate surface evaporation often lead to waterline recession; this recession may lead to greater sediment (i.e., playa) exposure and increased dust storm frequency (4). Waterline recession and consequential dust events emit insoluble minerals, organic compounds, microbial cells and spores, and microbial exudates, which may become concentrated prior to being aerosolized into local environments. This phenomenon can be harmful to public health; inhaling these increasingly concentrated aerosolized substances presents risks for residents and local communities in surrounding regions (3,5).

At the Salton Sea, a terminal lake located in California's Imperial Valley, ecological crises have led to a public health concern. The lake was once a popular destination for watersports and tourism, but now the degraded lake basin is notorious for its massive ecological die-offs and toxic marine environment (6). Agricultural waste dumping and a series of freshwater diversions (7) have left the Salton Sea heavily concentrated with unsafe levels of heavy metals, organic residues, and pesticides (8). Increasing regional temperatures and continually decreasing water inputs have led to the

lake's steady recession, transforming the previously submerged lake bottom into newly exposed playa (9). This concentrated, crust-like playa is vulnerable to aerosolization during dust events. Because of these aerosolized exposure risks, the Salton Sea has become a primary suspect for the region's disproportionately higher rates of asthma-related emergencies, as compared to the total population of California (10,11).

Inhaling dust-derived substances may damage lung health. During normal aspiration, foreign materials from the aeolian environment are consistently introduced into the mammalian respiratory tract (12). Human-host related mechanisms dispel these substances to prevent deep penetration into pulmonary systems. Mucociliary action, antimicrobial peptides, and innate or adaptive immunity contribute to proper clearance of these substances and other potentially harmful agents. However, increased agent frequency or load can overwhelm or bypass these mechanisms, which may result in pulmonary dysbiosis and cause respiratory distress upon inhalation.

In immunocompetent individuals, respiratory tracts are home to low-biomass microbial communities. Despite the tract having once been considered sterile, it is now suspected that microorganisms in the human respiratory tract result from incidental inhalation and micro-aspiration (13). While microbes in the upper respiratory tract (URT) have been found to support host clearance mechanisms and assist in defending against the burden of harmful foreign agents, the dispersion of microbes across the human airway may encourage niche partitioning, owing to either taxonomic, functional, or commensal activities (14). Metabolic and eco-physiological differences among microbial groups, including pathogenicity, as well as the importance of microbiomes for human physiology

and disease, underscore the need to consider microbiome composition within the respiratory tract in this system (1,15). Pathogenic potential, timing of microbial arrival, and competition may influence the lung microbiome structure and composition, especially in the lower respiratory tract (LRT), where the steady-state, low-level microbiome must withstand low nutrient supply, stringently high oxygen levels, and antibacterial host responses attributed to the innate immune system.

As the lung microbiome structure correlates with the development and regulation of host immune systems (13), lung microbiomes may directly influence or respond to host pulmonary diseases. Under various disease states, lung microbial composition and diversity shift in patients suffering from asthma, chronic obstructive pulmonary disease (COPD), and cystic fibrosis (16). However, it is not clear whether a host's lung microbiome profile can be used to explicitly differentiate between a healthy and diseased lung phenotype. While pulmonary inflammatory responses may correlate with compositional shifts in lung microbial communities, these responses may be contingent on temporal, climatic, and other external variables, including consistent exposure to environmental aerosols, as suspected among residents in and around the Salton Sea basin.

This study characterizes ambient lung microbiomes as compared to experimentally induced aerosolized dust exposures. We chronically exposed mice to dust collected near California's Salton Sea, which has been shown to trigger an acute innate immune response within the murine lung (17). Since short exposures to comparable desert dust collected further away from the Sea yielded attenuated immune responses (18), we experimented with dust collected at sites near and further from the Sea to

compare exposure impacts on lung microbiomes. Using our novel array of exposure chambers (19), we examined microbial communities in the lungs of mice exposed to dust as compared to mice inhaling filtered air.

Mouse models have been used to understand respiratory health issues because murine lungs can replicate important features of human lung disease pathophysiology; therefore, murine models can be used to observe effects on human lung health, dysbiosis, and responses to medical treatments of pulmonary diseases (20). Focusing on understanding host physiology associated with environmental exposures, prior murine work with C57BL/6 mouse models in this system characterized neurological and immune responses to inhaled vapors and aerosolized substances originating from the Salton Sea region (18,21). While neurological responses to inflammation may vary by mouse sex (22), pulmonary inflammatory responses did not vary by sex. Additionally, lung microbiomes of healthy, C57BL/6 mice may be susceptible to environmentally dependent convergence after at least seven days of co-housing (23). If our chamber experiments with C57BL/6 mice facilitate lung microbiome clustering among animals exposed to filtered air, then we would expect to observe similar compositional clustering among the lung microbiomes of dust-exposed mice. Likewise, if we observe convergent lung microbiome communities, then we hypothesize that there will be no detectable differences observed between right and left or partitioned lobes from the same animals. Moreover, dust exposure would affect mouse health and the composition of their lung microbiomes. If dust exposure alters health or microbiome status, then baseline lung microbiomes will be affected by chronic exposure to environmental aerosols;

furthermore, we hypothesize that these exposures will change lung microbial composition and diversity.

Previous host immunology studies revealed that chronic exposure to dust collected at the Salton Sea at different time points consistently elicits host pulmonary inflammation and other host responses (18), and these inflammatory responses were dissimilar to traditional allergic asthmatic cases. Due to the biochemical changes that occur during lung inflammation, we hypothesize that exposure-induced pulmonary inflammation, regardless of dust variability, will consistently alter lung microbial composition and diversity.

The public health crisis at the Sea corresponds with landscape level changes and increased dust promotion from this degraded ecosystem at the brink of collapse (24–26). The drying lake has the potential to emit toxic substances that may influence public health and host microbiome status. Moreover, as pollution and climate change weaken the resilience of terminal lakes such as the Great Salt Lake, the Aral Sea, and the Salton Sea, it is imperative to understand risks and support improved public health outcomes for inhabitants of these regions.

Materials and Methods

Salton Sea Dust Collection and Processing

Passive dust collectors (27) were deployed at two sites of varying distance to the Salton Sea perimeter (Fig. 1.1). The Palm Desert (PD) site (33°46'25.7"N

116°21'10.3"W) is located 25.5 miles from the lakebed's nearest waterline and serves as a geographic control site. Wister (WI) is a site (33°17'01.9"N 115°36'00.3"W) situated less than 2 miles off the southeastern edge of the Salton Sea, and dust from this site has consistently yielded histological inflammatory responses and exacerbated pulmonary health statuses in murine systems, as per Biddle et al. (18). We selected two deployment time points: August-October 2020 (WI2020) and September-December 2021 (WI2021, PD2021) because of previous illustrative and immunological analyses. The illustrative analyses showed higher levels of organic matter in Wister dust from these time points, supported by the immunological analyses.

After the deployment period, dust collectors were rinsed in MilliQ water and aqueous suspensions were filtered through 0.2 μM mesh. Aqueous filtrate was frozen then lyophilized before use in chamber exposure experiments. Because the gauge of the mesh was big enough to let water and minerals pass through, but too small to allow for microbial cells to pass through, the remaining lyophilized and concentrated filtrate should be mostly devoid of viable, intact, microbial cells. Subsequently, this concentrated filtrate was resuspended in MilliQ water before aerosolization.

Animal Use Ethics

Mice studies were performed in compliance with the University of California, Riverside's Institutional IACUC and NIH guidelines. Male and female, 8- to 9-week-old C57BL/6 mice were purchased from Jackson Labs (Sacramento, CA). Mice were

acclimated for approximately one week in a specific-pathogen free vivarium (University of California, Riverside) before use in our chamber exposure studies.

Chamber Exposures

Cages of 3-4 C57BL/6 mice were randomized between two 540L treatment chambers (exposed and control) modeled after those described in Peng et al. (19). Equal counts of male and female mice were distributed between the two treatment groups. Mice were kept in their respective chambers for 7 days with access to food and water, as needed.

For each experiment, the control chamber was filled with dry, filtered air; for the experimental dust manipulations, we mixed this filtered air with aerosolized filtrate suspension passed through a silica drying column as described in Biddle et al. (17). Filtrate concentration was maintained at approximately 1500 $\mu g/m^3$ over the experiment's entire duration. Control-air mice were used to define a "baseline" phenotype within the context of this study based on the expectation that this group would exhibit ambient inflammation in comparison to their relative dust-exposed treatment groups at the end of the 7-day exposure period.

Lower Respiratory Tract Dissection and Processing

At the end of the 7-day chamber exposure period, mice were euthanized with isoflurane and cervical dislocation, as per humane animal use protocols. Extraction of

LRT tissue was conducted at the mid-trachea for each animal, and lung lobes were separated at the tracheal bifurcation before storing at -80C for downstream use.

Additional lung tissues and bronchoalveolar lavage fluid (BALF) were collected for subsequent analysis of host immune response as described in Biddle et al., 2023 (18). BALF samples were stained with fluorescent antibodies: anti-CD45 FITC (BioLegend, San Diego, USA; Clone 30-F11), anti-CD19 PE-Cy5 (eBioscience, San Diego, USA; Clone MB19-1), anti-CD3 Alexa Fluor 700 (BioLegend, San Diego, USA; Clone 17A2), anti-Ly6G BV510 (BioLegend, San Diego, USA; Clone 1A8), anti-CD11b BV421 (BioLegend, San Diego, USA; Clone M1/70), anti-CD11c PE-Cy7 (BioLegend, San Diego, USA; Clone N418) and anti-SiglecF APC (BioLegend, San Diego, USA; Clone S17007L). Flow cytometry was performed on a MoFlo Astrios (Beckman Coulter, Carlsbad, CA) and gating and analysis were done using FlowJo (Version 10.71).

Lung Microbiome Library Prep and Sequencing

Microbial DNA from whole- or half-lung lobes was extracted using a HostZERO Microbial DNA extraction kit (Zymo Research, Irvine, CA) following a modified version of the manufacturer's protocol for solid tissue samples by disrupting these microbe-containing lung tissues. We performed tissue lysis using 2.0 mm beads on a MP Bio Fastprep Classic (MP Biomedicals, Irvine, CA) for one minute at maximum speed, followed by a 2-minute centrifugation cycle to separate eukaryotic and microbial components. After two subsequent cycles of mixing and centrifugation, we resuspended pellets and performed three incubations; the first was at 37 °C for 30 minutes, the second

included proteinase K treatments at 55 °C for 10 minutes, and the third incubation was at room temperature for 5 minutes. Next, we transferred solutions to lysis tubes containing 0.1 and 0.5 mm beads for five cycles of lysis and 5 minute incubations on ice, followed by centrifugation and downstream DNA extraction, as per the manufacturer's recommendation. However, we modified this protocol to maximize the microbial extraction process by transferring a total of 700 µl of supernatant into two parallel extractions from each of our whole- or half-lung samples, which we subsequently combined as a singular DNA template corresponding to that particular animal.

Due to the lungs being characterized by low microbial biomass, negative controls were used alongside DNA extractions to control for potential contaminants in downstream analyses. DNA extracts were quantified with Qubit (Invitrogen, Carlsbad, CA); double-stranded DNA mass (ng) concentrations from negative control samples were undetectable (per µl) in comparison to template from lung samples (23). Extracts with detectable DNA concentrations were sent to Zymo Research (Irvine, CA) for targeted-amplicon library preparation of 16S V3-V4 rRNA gene sequencing.

Prior to library preparation, a High Resolution Cleanup (HRC) PCR inhibitor removal step was conducted using the OneStep PCR Inhibitor Removal Kit (Zymo Research, Irvine, CA). Following this step, 16S rRNA amplification was done for the V3 and V4 regions using the Quick-16S NGS Library Prep Kit (Zymo Research, Irvine, CA) with added Peptide Nucleic Acids (PNAs; i.e., mitochondrial blockers), as per Lundberg et al. (28), to minimize the amplification of eukaryotic mitochondrial DNA. Negative controls were maintained throughout the amplification pipeline for tracking

contamination and protocol efficacy. Libraries were sequenced with an Illumina NextSeq 2000 using the p1 reagent kit (600 cycles) and a 30% PhiX spike to promote read diversity. Sequences were submitted to the National Center for Biotechnology Information Sequence Read Archive under BioProject PRJNA1124545.

Bioinformatics Amplicon Sequence Analysis

16S rRNA (V3 and V4) amplicon sequence data were analyzed using methods described in Freund, et al. (29,30). Sequence quality was assessed using FastQC and eestats2 (31). Sequences that passed through these quality thresholds were trimmed and ASVs were assigned using the DADA2 pipeline (32). The R "decontam" package was used to identify and remove amplicon sequencing variants (ASVs) associated with negative control samples and potential contaminants, as well as chloroplast or mitochondria-associated taxa.

Data Analysis and Statistics

All 16S rRNA amplicon sequencing data were analyzed in RStudio (R software version 3.18) using methods described in Freund et al. (2025). Normal distribution for Shannon-Weiner diversity and species richness among the lung microbiomes of exposure treatment groups were determined using the Shapiro-Wilks test. Since Shannon-Weiner diversity ($P<.001$) and species richness ($P<.001$) were not normally distributed, we used the Kruskal-Wallis test ("kruskal.test" function, "stats" package) to compare variance of

means for both Shannon-Weiner diversity and species richness between exposure treatment groups. If the variance within the means of Shannon-Weiner diversity or species richness differed significantly between groups (α=0.05), we performed a Dunn test ("dunn_test" function, "rstatix" package) to determine which pair(s) of exposure treatment groups differed in Shannon-Weiner diversity or taxa richness.

The R "vegan" package was used for beta diversity. Data was transformed by center-log ratio (CLR) with the "decostand" function, and a Principal Coordinates Analysis (PCoA) was performed and visualized on Aitchison distances (33–35). Before pairwise comparisons were run, "betadisper" was used to assess homogeneity of variance. After ensuring that dispersion did not differ significantly between groups, permutational multivariate analysis of variance (PERMANOVA) was performed using "adonis2," and comparisons between single pairings were clarified with "pairwiseAdonis" (36).

Results

Host Inflammatory Response, Lung Microbiome Composition, and Dust Exposure

We found that exposure to environmental dust elicits significant neutrophilic inflammation in mouse lungs when compared to their contemporaneous, ambient air control group (Fig. 1.2). Using a Kruskal-Wallis test for non-normally distributed data, we found that average neutrophil recruitment as a percentage of CD45+ cells differed significantly among treatment groups (P=0.004). A Wilcoxon test verified significant

increases in neutrophil percentages in PD2021 dust (P=0.029) and WI2020 dust (P=0.029) exposed mice, and a marginally significant increase in neutrophil recruitment in animals exposed to WI2021 dust (P=0.057) as compared to their contemporaneous controls. For mice exposed to WI2020 dust, average neutrophil recruitment was significantly higher than in mice exposed to PD2021 dust (P=0.029) or WI2021 dust (P=0.029), indicating a higher magnitude of neutrophilic pulmonary inflammation elicited by dust collected in fall of 2020 at the Wister site (close to the Salton Sea; WI2020). In contrast, no significant differences in eosinophil recruitment were observed among dust-exposure groups and their contemporaneous controls.

In terms of host neutrophil recruitment, control-air-exposed mice were deemed healthy, and were used to characterize a baseline lung microbiome within a shared environment. Using Aitchison distance matrices, we used a Principal Coordinates Analysis (PCoA) to visualize dissimilarities in lung microbial community composition by treatment group, such as exposure treatment (Fig. 1.3). Lung microbiomes of PD2021-, WI2020-, and WI2021-exposed mice have more dispersion than control-air-exposed mice. Moreover, the lung microbiomes of mice exposed to PD2021 dust cluster closely to mice exposed to ambient air, while microbiomes of mice exposed to WI2020 and WI2021 dust cluster further away from this group and each other. A PERMANOVA revealed that lung microbiome community composition significantly differed between exposure treatment groups (P<0.001). Specifically, exposure to WI2021 dust significantly changed lung microbiome composition in comparison to their contemporaneous control-air microbiomes (P=0.002). While exposure to PD2021 dust did not significantly change

lung microbiome composition in comparison to its contemporaneous control group (P=0.630), the composition of PD-exposed dust lung microbiomes differed significantly from WI2020 dust (P=0.003) and WI2021 dust (P=0.002) microbiomes. Likewise, lung microbiome composition in the WI2020-exposed group differed significantly from lung microbiomes associated with the WI2021-exposed group (P=0.002).

Baseline Lung Microbial Diversity and Dust Exposure

We calculated species richness and Shannon-Weiner diversity of lung microbial communities and used Kruskal-Wallis tests for determining differences between treatment groups (Fig. 1.4). Species richness did not differ significantly between groups (P=0.26). Likewise, Shannon-Weiner diversity did not differ significantly in dust-exposed lung microbiomes when compared to their contemporaneous ambient air controls (PD2021 P=0.95, WI2020 P=0.078, WI2020 P=0.23) When comparing Shannon-Weiner diversity between dust-exposed groups, lung microbiome diversity in WI2020-exposed mice did not differ significantly from that of PD2021-exposed mice (P=0.21). In contrast, Shannon-Weiner diversity differed significantly between WI2020- and WI2021-exposed mice (P<0.001), ostensibly because of variability in evenness across these two Wister-dust-exposed groups.

We used core microbiome analysis (37) to visualize evenness and taxa prevalence in each treatment group at a minimum threshold of 1% relative abundance (RA; Fig. 1.5). Species evenness was significantly different among groups according to exposure

material (P<0.01) with WI2021-exposed lung microbiomes being significantly less even compared to control air microbiomes (P=0.034) and WI2020-exposed lung microbiomes (P=0.006). When comparing lung microbiome taxa abundance between control-air- and dust-exposed mice, the WI2020 group displayed higher taxa abundance, with more or different taxa being uniquely present or more prevalent at 1% RA. These taxa include *Achromobacter*, *Atopostipes, Enhydrobacter, Methylobacterium, Methylorubrum,* and *Microbacterium*. In contrast, two taxa, *Paenarthrobacter* and *Staphylococcus,* were prevalent among 75-100% of WI2021 lung microbiome samples. Moreover, the WI2021-exposed group displayed lower abundances across core taxa, with most taxa being prevalent at approximately 25% of sampled lungs.

We used PERMANOVA to assess if differences in lung microbiome responses following chronic dust exposure could be attributed to mouse sex or lung lobe section (left vs. right lobe). We did not detect any effects due to sex or lobes. Among control-air-exposed mice only, no significant differences in baseline lung microbiome composition were attributed to either sex (P=0.567) or lobe section (P=0.721). Similarly, among dust-exposed mice only, no significant differences were detected in lung microbiome composition between sexes (P=0.848) or lobe sections (P=0.906).

Discussion

In this study, we showed that lung microbial community composition varied by dust exposure. Neutrophil recruitment was found to be higher in the lungs of dust-exposed mice compared to mice exposed to ambient filtered air. We characterized a baseline lung microbiome among mice used in this study; however, the specific

microbiome here described is not broadly indicative of host pulmonary health or inflammatory state beyond the scope of this study. While no differences in lung microbial communities were detected by mouse sex or lung lobe, the core lung microbiome diversity and composition were affected by dust source and exposure. Indeed, mice exposed to dust collected at the Wister site, which elicited a heightened neutrophilic immune response were characterized by higher beta- and alpha-diversity and evenness in their lung microbiomes than were Wister dust-exposed mice exhibiting lesser neutrophil recruitment. Likewise, dust from Wister exerts an influence on dust microbial composition and changes the relative abundance of prevalent taxa. Mouse lungs exposed to dust from Palm Desert, which is further from the Sea, were more similar to lungs from ambient control air exposures. Conversely, exposures to dust collected near the Sea from the Wister site in 2021 yielded lung microbiomes that clustered further from lungs exposed to ambient air.

Neutrophil recruitment differed between control and exposed groups, which suggests that chronic dust exposure does elicit neutrophilic inflammation; however, the magnitude of that inflammation is not consistent with the changes in lung microbiome diversity and composition. This suggests that the host lung microbiome is responding directly to dust exposure rather than the physiological effects of lung inflammation. It is unclear if changes to lung architecture during disease drive lung microbial dysbiosis, or if dysbiosis instigates inflammation. Previous studies suggest that the lung microbiome profile and its relationship to the host's immune response is contingent on endotype (38). One study observed a lack of relationship between Type 2 asthma inflammatory markers

and lung microbiome composition but went on to suggest that dysbiosis in the lung microbiome could be highly relevant in patients with severe, non-Type 2 asthma (characterized by neutrophil-dominant inflammation), akin to what we have observed in this study (39). Furthermore, another study observed significantly higher bacterial species richness in asthma patient sputum samples characterized by mixed (neutrophil and eosinophil) or neutrophil-dominant endotypes when compared to eosinophil-dominant and paucigranulocytic endotypes (40). In our study, chronic exposure to abiotic dust material led to significant neutrophil-dominant inflammation when compared to their contemporaneous ambient air controls. Upon referencing significant changes observed in lung microbiome composition (Fig. 1.3), our findings suggest that dust-induced dysbiosis in the lung microbiome resulting from chronic exposure may be driving neutrophil recruitment and thus triggering significant pulmonary inflammation.

Host inflammatory response and lung microbiome composition are independently affected by chronic dust exposure. Previous studies show that low microbial diversity is related to poor lung function (41–44). Likewise, lung microbiomes in children with asthma may be composed differently than healthy children's lungs (45), which could relate to disease severity or type of medical intervention. Our study found that while chronic dust exposure altered lung microbiome diversity, it did so independently from host pulmonary inflammatory state.

Although microbial taxa richness did not vary, baseline lung microbiome diversity changed from chronic exposure to Wister dust. Mouse lungs exposed to dust from Wister collected in 2020 were as diverse as Palm Desert (2021)-exposed mouse lungs. However,

the mouse lungs exposed to dust from Wister in 2021 surpassed microbial diversity levels of the other treatment groups. Given that dust storms entrain microbial residues, chemical constituents, and particulates that could result in host responses to that dust, the presence or prevalence of these substances likely changes the relative abundance of taxa found in lung microbiomes. Previous studies show that exposure to particulate matter, dust, smoke, or ozone can lead to lung microbial dysbiosis, which may be related to asthmatic inflammation or other respiratory pathologies (46,47). Yet data from several of these studies are correlative and are apt to raise more questions about whether the substances alter lung microbiomes directly or lung injury following exposure to these types of residues or substances alters the respiratory ecosystem, thereby impacting the microbiome indirectly. Our study showed higher evenness in mouse lungs exposed to dust from Wister in 2020 than other dust sources or dates, which contributed to the heightened diversity detected in these lung microbiomes.

We detected higher prevalence of Gram-positive bacteria *Paenarthrobacter* and *Staphylococcus* in lungs exposed to dust from Wister collected in 2021, which were common across animals in that treatment group and correlated with lower neutrophil recruitment. In contrast, the lungs exposed to dust from Wister in 2020 had higher neutrophil recruitment and more Gram-negative *Pseudomonas* spp. than lungs exposed to WI2021 dust. In contrast to our finding that lungs enriched in *Pseudomonas* harbored high microbial diversity, previous work on *Pseudomonas aeruginosa* found correlations with *Pseudomonas* and decreased lung microbial diversity (48–50). *Pseudomonas* has been commonly found in patients' lungs with severe asthmatic inflammation (51,52), yet

Pseudomonas is virtually undetectable in normal healthy lungs. Other studies suggest that neutrophil recruitment and host inflammatory response may generally relate to Gram-negative bacteria, like *Pseudomonas,* that are enriched with lipopolysaccharides (LPS) and mediate neutrophil activation. Likewise, our findings showed more prevalent Gram-negative taxa in lung microbial communities exposed to WI2020 dust than were found in WI2021-exposed lungs. While different diseases, including asthma, may alter lung microbiome structure and function, other demographic features (such as age and gender) could determine whether exposed residents in the Salton Sea region would be susceptible to cardiopulmonary or neurological disease (53–55). Our study suggests that exposure to dust could influence lung microbiome structure in vulnerable populations.

Overall, our findings show that environmental dust exposure changes lung microbial communities. Given the predicted increase in Salton Sea dust emissions, entrained dust may introduce contaminants, minerals, and other potential toxins into the atmosphere. These changing conditions may also influence the geographic distribution and functional capacity of aeolian microbial community originating from the drying Salton Sea lakebed. However, our study utilized filtered, abiotic dust material and thus, does not represent the direct effects of the Salton Sea aeolian microbiome on host lung microbiome composition. Altogether, microbial residues, chemical constituents, along with mineral and organic particulates in local dust emissions can compound exposure risks for the region's inhabitants, as well as have implications for ecosystem stability, conservation, and public health.

List of Figures

Figure 1.2 Map of Salton Sea and dust collection sites. Wister (WI, red) is located < 2mi from the eastern edge of the Salton Sea. Palm Desert (PD) is located approximately 26mi northwest from the Salton Sea. Dust material from Boyd Deep Canyon (BDC) was used in previous host pulmonary inflammation studies (18), and is a site located approximately 20mi northwest from the Salton Sea.

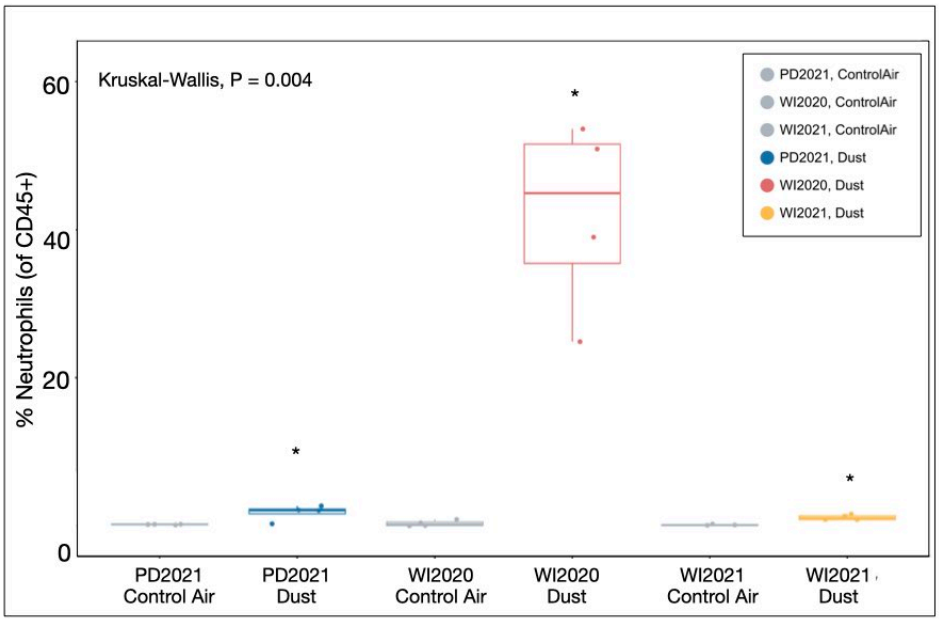

Figure 1.3 Inflammatory responses to dust exposure. Average neutrophil recruitment (% of CD45+ cells) in mouse lungs differed significantly by exposure material (P=0.004). Neutrophil recruitment was significantly higher in dust-exposed lungs when compared to their contemporaneous controls.

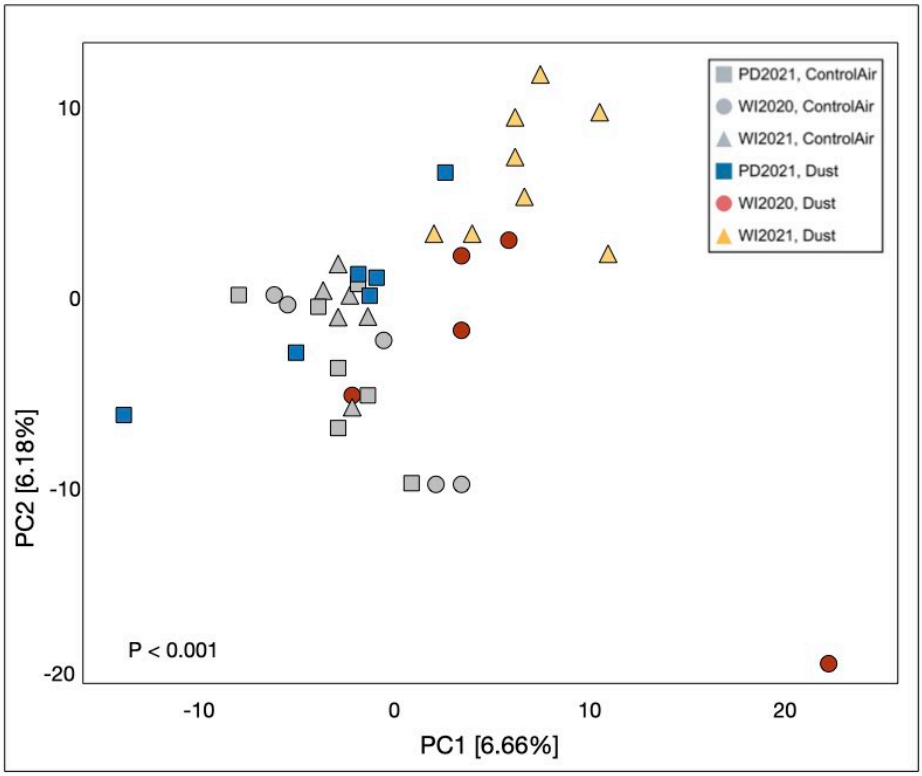

Figure 1.4 Microbial community composition in exposed mouse lungs. Lung microbial community composition differs significantly among exposure material groups ($P<0.001$). Microbiomes of mice exposed to PD2021 dust cluster closely to mice exposed to ambient air, while microbiomes of mice exposed to WI2020 and WI2021 dust cluster separately from this group and each other. Overall, dust-exposed microbiomes are more widely dispersed than controls.

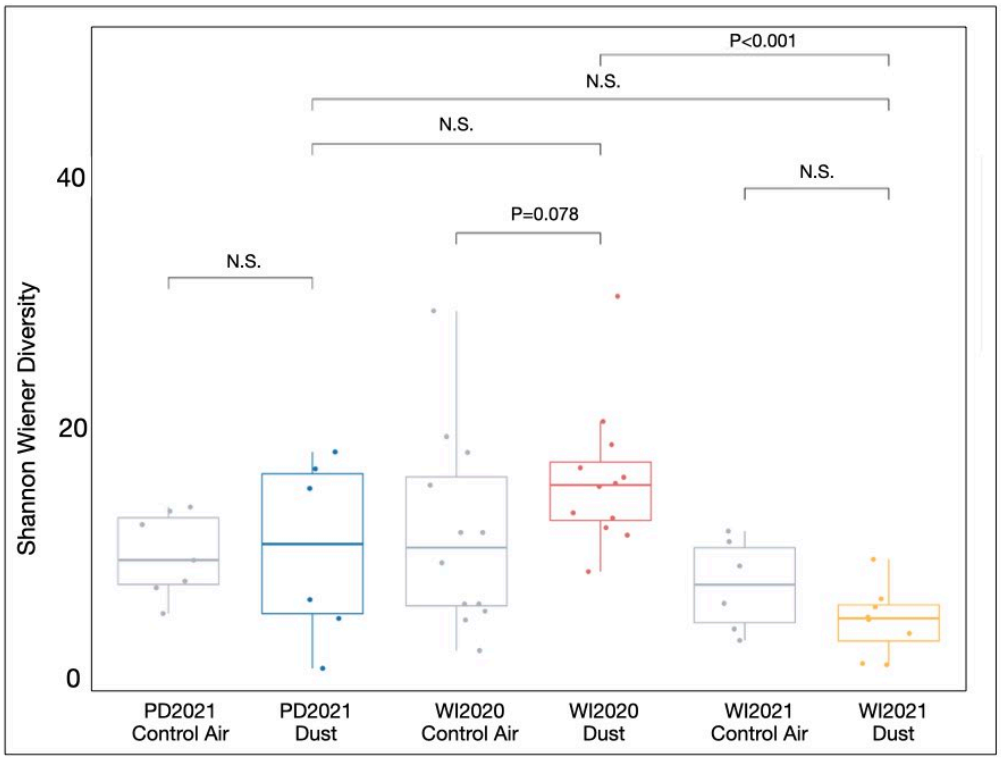

Figure 1.5 Microbial diversity varies by dust exposure. While average Shannon-Weiner diversity differs significantly among exposure groups (P=0.0027), dust exposures do not differ significantly from their contemporaneous controls. Average Shannon-Weiner diversity is significantly higher in WI2020-exposed lung microbiomes compared to WI2021-exposed lung microbiomes.

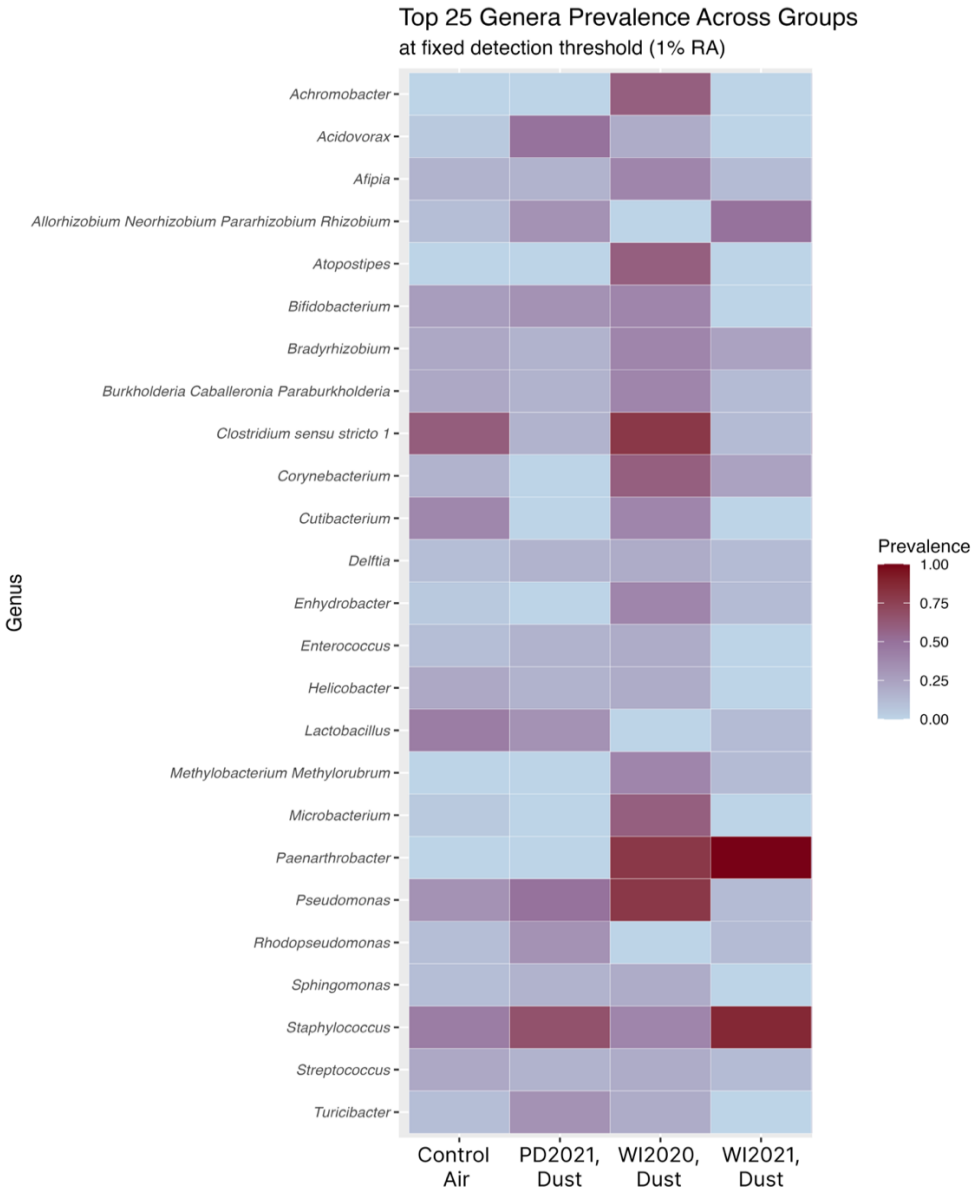

Figure 1.6 Prevalent microbial genera across treatment groups. Prevalence is calculated as a percentage of the samples where the taxa are observed at 1% relative abundance or higher. In control air-exposed lung microbiomes, most taxa are moderately prevalent (25-75%). In WI2021-exposed lung microbiomes, few taxa are represented at high (>75%) prevalence, while many other taxa are represented at low (<25%) prevalence.

References

1. Maltz MR, Carey CJ, Freund HL, Botthoff JK, Hart SC, Stajich JE, et al. Landscape Topography and Regional Drought Alters Dust Microbiomes in the Sierra Nevada of California. Front Microbiol. 2022 Jun 28;13:856454.

2. Yamaguchi N, Park J, Kodama M, Ichijo T, Baba T, Nasu M. Changes in the Airborne Bacterial Community in Outdoor Environments following Asian Dust Events. Microbes Environ. 2014;29(1):82–8.

3. Esmaeil N, Gharagozloo M, Rezaei A, Grunig G. Dust events, pulmonary diseases and immune system. 2014 Mar 15;

4. Zucca C, Middleton N, Kang U, Liniger H. Shrinking water bodies as hotspots of sand and dust storms: The role of land degradation and sustainable soil and water management. CATENA. 2021 Dec;207:105669.

5. Cook AG, Weinstein P, Centeno JA. Health Effects of Natural Dust: Role of Trace Elements and Compounds. Biol Trace Elem Res. 2005;103(1):001–16.

6. Cohen MJ, Morrison JI, Glenn EP. The Ecology and Future of the Salton Sea. 1999 Feb;

7. Johnston JE, Razafy M, Lugo H, Olmedo L, Farzan SF. The disappearing Salton Sea: A critical reflection on the emerging environmental threat of disappearing saline lakes and potential impacts on children's health. Sci Total Environ. 2019 May;663:804–17.

8. Moreau MF, Surico-Bennett J, Vicario-Fisher M, Gerads R, Gersberg RM, Hurlbert SH. Selenium, arsenic, DDT and other contaminants in four fish species in the Salton Sea, California, their temporal trends, and their potential impact on human consumers and wildlife. Lake Reserv Manag. 2007 Dec;23(5):536–69.

9. Jones BA, Fleck J. Shrinking lakes, air pollution, and human health: Evidence from California's Salton Sea. Sci Total Environ. 2020 Apr;712:136490.

10. Farzan SF, Razafy M, Eckel SP, Olmedo L, Bejarano E, Johnston JE. Assessment of Respiratory Health Symptoms and Asthma in Children near a Drying Saline Lake. Int J Environ Res Public Health. 2019 Oct 11;16(20):3828.

11. Miao Y, Porter WC, Schwabe K, LeComte-Hinely J. Evaluating health outcome metrics and their connections to air pollution and vulnerability in Southern California's Coachella Valley. Sci Total Environ. 2022 May;821:153255.

12. Whiteson KL, Bailey B, Bergkessel M, Conrad D, Delhaes L, Felts B, et al. The Upper Respiratory Tract as a Microbial Source for Pulmonary Infections in Cystic

Fibrosis. Parallels from Island Biogeography. Am J Respir Crit Care Med. 2014 Jun 1;189(11):1309–15.

13. Marimón JM. The Lung Microbiome in Health and Respiratory Diseases. Clin Pulm Med. 2018 Jul;25(4):131–7.

14. Hamm PS, Taylor JW, Cook JA, Natvig DO. Decades-old studies of fungi associated with mammalian lungs and modern DNA sequencing approaches help define the nature of the lung mycobiome. Sheppard DC, editor. PLOS Pathog. 2020 Jul 30;16(7):e1008684.

15. Blaser MJ. The microbiome revolution. J Clin Invest. 2014 Oct 1;124(10):4162–5.

16. Dickson RP, Erb-Downward JR, Martinez FJ, Huffnagle GB. The Microbiome and the Respiratory Tract. Annu Rev Physiol. 2016 Feb 10;78(1):481–504.

17. Biddle TA, Li Q, Maltz MR, Tandel PN, Chakraborty R, Yisrael K, et al. Salton Sea aerosol exposure in mice induces a pulmonary response distinct from allergic inflammation. Sci Total Environ. 2021 Oct;792:148450.

18. Biddle TA, Yisrael K, Drover R, Li Q, Maltz MR, Topacio TM, et al. Aerosolized aqueous dust extracts collected near a drying lake trigger acute neutrophilic pulmonary inflammation reminiscent of microbial innate immune ligands. Sci Total Environ. 2023 Feb;858:159882.

19. Peng X, Maltz MR, Botthoff JK, Aronson EL, Nordgren TM, Lo DD, et al. Establishment and characterization of a multi-purpose large animal exposure chamber for investigating health effects. Rev Sci Instrum. 2019 Mar 1;90(3):035115.

20. Rydell-Törmänen K, Johnson JR. The Applicability of Mouse Models to the Study of Human Disease. In: Bertoncello I, editor. Mouse Cell Culture [Internet]. New York, NY: Springer New York; 2019 [cited 2025 Mar 5]. p. 3–22. (Methods in Molecular Biology; vol. 1940). Available from: http://link.springer.com/10.1007/978-1-4939-9086-3_1

21. Llamas MJV. Adult mice exposed to aerosolized Alternaria exhibit neuroinflammation in the brainstem but not rest of brain. 2016.

22. Paolicelli RC, Sierra A, Stevens B, Tremblay ME, Aguzzi A, Ajami B, et al. Microglia states and nomenclature: A field at its crossroads. Neuron. 2022 Nov;110(21):3458–83.

23. Dickson RP, Erb-Downward JR, Falkowski NR, Hunter EM, Ashley SL, Huffnagle GB. The Lung Microbiota of Healthy Mice Are Highly Variable, Cluster by

Environment, and Reflect Variation in Baseline Lung Innate Immunity. Am J Respir Crit Care Med. 2018 Aug 15;198(4):497–508.

24. Freund H, Maltz MR, Swenson MP, Topacio TM, Montellano VA, Porter W, et al. Microbiome interactions and their ecological implications at the Salton Sea. Calif Agric. 2022 Apr;76(1):16–26.

25. Miao Y, Porter WC, Benmarhnia T, Lowe C, Lyons TW, Hung C, et al. Source-specific acute cardio-respiratory effects of ambient coarse particulate matter exposure in California's Salton Sea region. Environ Res Health. 2025 Mar 1;3(1):015006.

26. Sinclair RG, Gaio J, Huazano SD, Wiafe SA, Porter WC. A Balloon Mapping Approach to Forecast Increases in PM10 from the Shrinking Shoreline of the Salton Sea. Geographies. 2024 Oct 17;4(4):630–40.

27. Aciego SM, Riebe CS, Hart SC, Blakowski MA, Carey CJ, Aarons SM, et al. Dust outpaces bedrock in nutrient supply to montane forest ecosystems. Nat Commun. 2017 Mar 28;8(1):14800.

28. Lundberg DS, Yourstone S, Mieczkowski P, Jones CD, Dangl JL. Practical innovations for high-throughput amplicon sequencing. Nat Methods. 2013 Oct;10(10):999–1002.

29. Freund L, Hung C, Topacio TM, Diamond C, Fresquez A, Lyons TW, et al. Diversity of sulfur cycling halophiles within the Salton Sea, California's largest lake. BMC Microbiol. 2025 Mar 6;25(1):120.

30. Maltz MR, Allen MF, Phillips ML, Hernandez RR, Shulman HB, Freund L, et al. Microbial community structure in recovering forests of Mount St. Helens. Front Microbiomes. 2024 Nov 4;3:1399416.

31. Andrews S. Andrews S. FastQC: A Quality Control Tool for High Throughput Sequence Data. 2010. [Internet]. 2010. Available from: https://www.bioinformatics.babraham.ac.uk/projects/fastqc/

32. Callahan BJ, McMurdie PJ, Rosen MJ, Han AW, Johnson AJA, Holmes SP. DADA2: High-resolution sample inference from Illumina amplicon data. Nat Methods. 2016 Jul;13(7):581–3.

33. Lubbe S, Filzmoser P, Templ M. Comparison of zero replacement strategies for compositional data with large numbers of zeros. Chemom Intell Lab Syst. 2021 Mar;210:104248.

34. Quinn TP, Erb I, Richardson MF, Crowley TM. Understanding sequencing data as compositions: an outlook and review. Wren J, editor. Bioinformatics. 2018 Aug 15;34(16):2870–8.

35. Quinn TP, Erb I, Gloor G, Notredame C, Richardson MF, Crowley TM. A field guide for the compositional analysis of any-omics data. GigaScience. 2019 Sep 1;8(9):giz107.

36. Martinez Arbizu P. pairwiseAdonis [Internet]. 2020. Available from: https://github.com/pmartinezarbizu/pairwiseAdonis

37. Lahti L, Shetty S. Core microbiome [Internet]. 2018. Available from: https://microbiome.github.io/tutorials/Core.html

38. Natalini JG, Singh S, Segal LN. The dynamic lung microbiome in health and disease. Nat Rev Microbiol. 2023 Apr;21(4):222–35.

39. Huang YJ, Charlson ES, Collman RG, Colombini-Hatch S, Martinez FD, Senior RM. The Role of the Lung Microbiome in Health and Disease. A National Heart, Lung, and Blood Institute Workshop Report. Am J Respir Crit Care Med. 2013 Jun 15;187(12):1382–7.

40. Son JH, Kim JH, Chang HS, Park JS, Park CS. Relationship of Microbial Profile With Airway Immune Response in Eosinophilic or Neutrophilic Inflammation of Asthmatics. Allergy Asthma Immunol Res. 2020;12(3):412.

41. Coburn B, Wang PW, Diaz Caballero J, Clark ST, Brahma V, Donaldson S, et al. Lung microbiota across age and disease stage in cystic fibrosis. Sci Rep. 2015 May 14;5(1):10241.

42. Cox MJ, Allgaier M, Taylor B, Baek MS, Huang YJ, Daly RA, et al. Airway Microbiota and Pathogen Abundance in Age-Stratified Cystic Fibrosis Patients. Ratner AJ, editor. PLoS ONE. 2010 Jun 23;5(6):e11044.

43. Flight WG, Smith A, Paisey C, Marchesi JR, Bull MJ, Norville PJ, et al. Rapid Detection of Emerging Pathogens and Loss of Microbial Diversity Associated with Severe Lung Disease in Cystic Fibrosis. McAdam AJ, editor. J Clin Microbiol. 2015 Jul;53(7):2022–9.

44. Hahn A, Warnken S, Pérez-Losada M, Freishtat RJ, Crandall KA. Microbial diversity within the airway microbiome in chronic pediatric lung diseases. Infect Genet Evol. 2018 Sep;63:316–25.

45. Hilty M, Burke C, Pedro H, Cardenas P, Bush A, Bossley C, et al. Disordered Microbial Communities in Asthmatic Airways. Neyrolles O, editor. PLoS ONE. 2010 Jan 5;5(1):e8578.

46. Hosang L, Canals RC, Van Der Flier FJ, Hollensteiner J, Daniel R, Flügel A, et al. The lung microbiome regulates brain autoimmunity. Nature. 2022 Mar 3;603(7899):138–44.

47. Utembe W, Kamng'ona AW. Inhalation exposure to chemicals, microbiota dysbiosis and adverse effects on humans. Sci Total Environ. 2024 Dec;955:176938.

48. Carmody LA, Zhao J, Schloss PD, Petrosino JF, Murray S, Young VB, et al. Changes in Cystic Fibrosis Airway Microbiota at Pulmonary Exacerbation. Ann Am Thorac Soc. 2013 Jun;10(3):179–87.

49. Fodor AA, Klem ER, Gilpin DF, Elborn JS, Boucher RC, Tunney MM, et al. The Adult Cystic Fibrosis Airway Microbiota Is Stable over Time and Infection Type, and Highly Resilient to Antibiotic Treatment of Exacerbations. Fleiszig S, editor. PLoS ONE. 2012 Sep 26;7(9):e45001.

50. Zemanick ET, Rosas-Salazar C. The Role of the Microbiome in Pediatric Respiratory Diseases. Clin Chest Med. 2024 Sep;45(3):587–97.

51. Li R, Li J, Zhou X. Lung microbiome: new insights into the pathogenesis of respiratory diseases. Signal Transduct Target Ther. 2024 Jan 17;9(1):19.

52. Lyon J. The Lung Microbiome: Key to Respiratory Ills? JAMA. 2017;317:1713–4.

53. Cole TB, Coburn J, Dao K, Roqué P, Chang YC, Kalia V, et al. Sex and genetic differences in the effects of acute diesel exhaust exposure on inflammation and oxidative stress in mouse brain. Toxicology. 2016 Dec;374:1–9.

54. da Silva Frost P. Sex Specific Mechanisms of Disease: Crosstalk Between Brain and Periphery in Inflammation [Internet]. [Riverside]: UC Riverside; 2023. Available from: https://www.proquest.com/docview/2842739982?pq-origsite=gscholar&fromopenview=true&sourcetype=Dissertations%20&%20Theses

55. Valdez JM. Systemic Inflammation Affects the CNS in an Age, Duration, and Sex Dependent Man [Internet] [Dissertation]. [Riverside]: UC Riverside; 2021. Available from: https://escholarship.org/uc/item/72d9f91x

Supplementary Materials

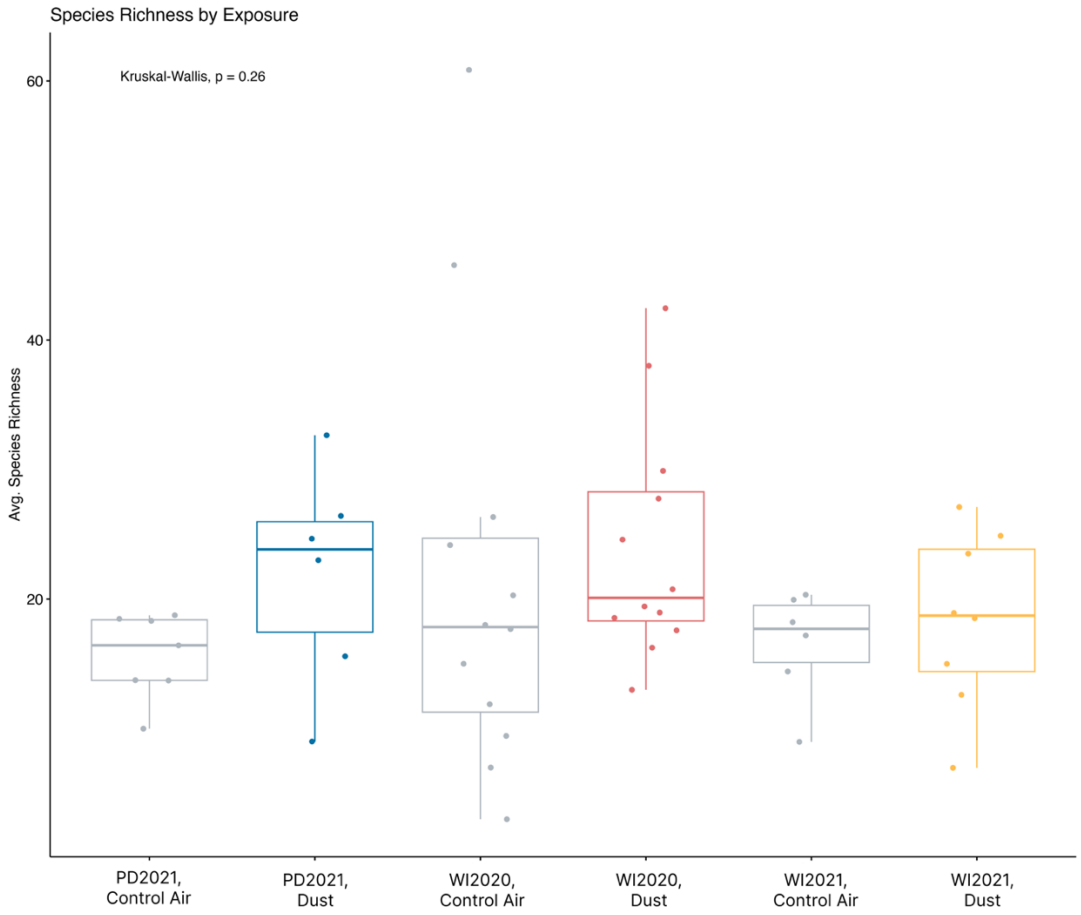

S1.1. Microbial species richness and dust exposure. Average species richness does not differ significantly among exposure groups (P=0.26).

CHAPTER II

Title: Spatiotemporal Variation of Salton Sea Dusts Differentially Affect The Lung Microbiome

Abstract

Lung microbiome composition and diversity may be significantly altered by chronic exposure to Salton Sea dust. To further scrutinize these findings, we hypothesize that spatiotemporal variation in Salton Sea dust composition leads to differential impacts on lung microbiome diversity and composition after exposure. We utilized dust collected at three different sites around the Salton Sea and for each site; at least two collection periods from the summer to late fall of 2020, 2021, and 2022 were represented. Filtered dust was used for 7-day chronic exposures in controlled mouse chambers after which lung and fecal samples were used for 16s rRNA V3-V4 amplicon sequencing. We verified that chronic exposure to dust elicits neutrophilic pulmonary inflammation, especially among mice exposed to dust collected at the Wister site, close to the Salton Sea. We found that spatiotemporal variation significantly motivated variation in lung microbiome composition in 2022 dust-exposed mice. The lung microbiomes of dust-exposed mice were found to increase in diversity and richness, while simultaneously decreasing in evenness. In contrast, the fecal microbiomes of dust-exposed mice decreased in diversity and richness. Our findings suggest that chronic exposure to dust collected at Wister, a site near the Salton Sea, triggers a systemic stress response in mice characterized by high neutrophil recruitment, increased lung microbiome diversity, and subsequently decreased fecal microbiome diversity. These findings, however, do not exactly align with any singular lung microbiome-disease phenotype, demonstrating the variable capacity of environmental dust exposure to elicit health consequences relative to seasonal weather events.

Graphical Abstract

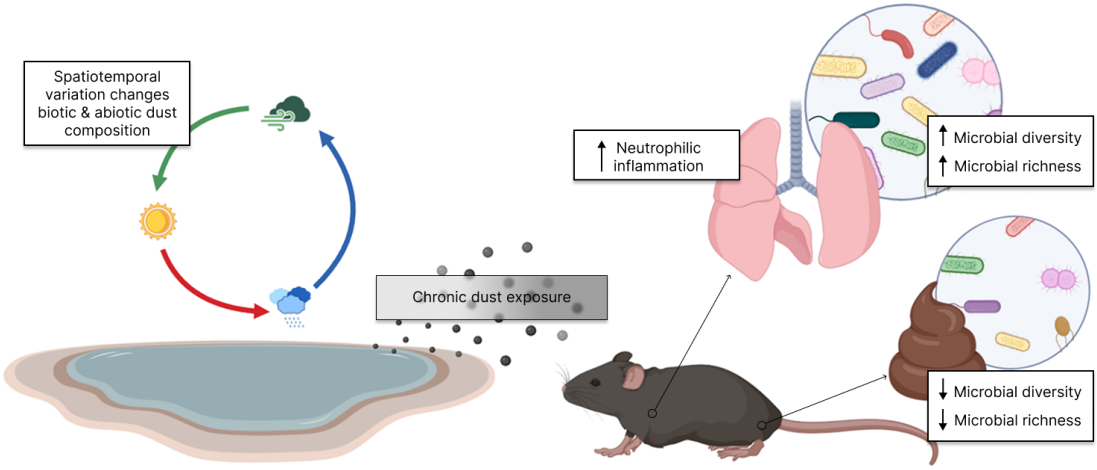

Introduction

We are consistently interacting with environmental microbes. Even in the built environment, where infrastructure has been specifically designed to filter air and limit our contact with infectious pathogens, interactions with high-traffic surfaces, plants, animals, and other humans define the microbial community we are exposed to on a daily basis (1). Recent popularization around the 'hygiene hypothesis' and gut microbiome research have brought attention to the symbiotic potential of microbes and thus, mediated positive associations with environmentally derived microbes. In the rural environment, however, the consequences of climate change and ecological negligence are mediating dramatic shifts to ecosystem stability (2,3). As temperatures become more extreme and natural resources are spent, restructuring of the macroenvironment has been shown to result in similar consequences for the environmental microbiome (4–7). While limited infrastructure and restorative resources in these regions make them more vulnerable to rapid ecological degradation, worsening climate stress will have broad and inevitable consequences across environments.

At California's Salton Sea basin, the terminal inland lakebed has been deprived of fresh input from the Colorado River, trading it for an influx of agricultural runoff from the Alamo, New, and Whitewater rivers (8). Eutrophication has resulted in frequent algal and gypsum blooms, fatally affecting local fish and migratory bird populations. Moreover, rising temperatures in the region have exacerbated the Salton Sea's receding waterline, and as more playa is exposed around its perimeter, regional dust events have become a greater concern among local residents who suffer from disproportionately

higher rates of asthma per capita when compared to California's total population (2,9–11).

Our preliminary work has begun to elucidate the relationship between the basin's changing ecology and the aeolian microbiome. Site by season variation in precipitation, UV, nutrient availability, as well as wind speed and directionality, are influential to local dust microbiome composition. Additionally, biogeochemical cycling in the lake itself significantly restructures microbial diversity in the water column, presenting an opportunity for unique microbes to be entrained in seaspray or playa derived aerosols (12). As a result of biogeochemical cycling, nutrient availability, and subsequent reassembly of environmental microbiomes, the abiotic composition of dust in the Salton Sea basin can vary from season to season (13).

We found that lung microbiome composition was significantly altered by chronic exposure to Salton Sea dust (14). As described above, seasonal variation at the Salton Sea basin definitively alters local dust and water microbiomes, coupled with shifts in the biogeochemistry of these substrates. This chapter builds on these findings as we hypothesize that variation in Salton Sea dust composition across sites and seasons leads to differential impacts on lung microbiome diversity and composition following chronic exposure.

We also predict that lung microbiome composition may be independently manipulated by direct dust exposure, rather than by host pulmonary inflammation and subsequent changes to lung physiology. While it is understood that the lung microbiome is closely associated with the development and function of the host immune system (15),

systemic influence of the lung microbiome is less realized. In contrast, the highly metabolic gut microbiome is known to augment proper immune function in the lung via microbially derived signaling molecules and taxa functionality (16,17). Due to the systemic significance of the gut microbiome and its indirect relationship with the aerosol environment (unlike the lung), we hypothesize that changes in the fecal microbiome of Salton Sea dust-exposed hosts will reflect inflammatory responses rather than variation in dust composition.

Ecological changes have been shown to impact public health in diverse contexts, including dramatic shifts in living environments, seasonal temperature fluctuations, and resource availability driven by climate change (18). However, the cascading effects of ecological distress on both environmental microbiomes and those of resident communities remain widely uncharacterized. This chapter explores how site-by-season variation in Salton Sea dust may influence lung microbiome diversity and composition following chronic exposure.

Methods

Salton Sea Dust Collection and Processing

Passive dust collectors (19) were deployed at three sites of varying distance to the Salton Sea (Fig. 2.1) during the fall of 2020, 2021, and 2022. Dust collectors at Palm Desert (PD, 33°46'25.7"N 116°21'10.3"W) were located 25.5 miles northwest from the lakebed's nearest waterline and were deployed from September 2021-March 2022 and June-September 2022. PD dust exposure has been previously associated with minimal

host pulmonary inflammation and minimal influence on mouse lung microbiome composition (20,21). Dust collectors at Wister (WI, 33°17'01.9"N 115°36'00.3"W) were located less than 2 miles off the southeastern edge of the Salton Sea and were deployed from August-October 2020, September-December 2021, and June-September 2022. Exposure to WI dust has been shown to significantly increase host neutrophil recruitment and influence the composition of the mouse lung microbiome. Dust collectors at the Agricultural site (AG, 33°10'07.9"N 115°51'21.8"W) were located less than 2 miles off the southwestern edge of the Salton Sea. These collectors were deployed from September-December 2021 and June-September 2022. Despite being as close to the Salton Sea as WI, preliminary AG dust experiments have not displayed consistent inflammatory effects on exposed mice.

Following the deployment period, dust collectors were rinsed in MilliQ water. The resulting aqueous suspensions were vacuum filtered through a 0.2 μM mesh to allow water-soluble components and minerals to pass through while blocking viable, in-tact microbial cells and large particles. The remaining filtrate was frozen and lyophilized to concentrate, then resuspended in MilliQ water before aerosolization.

Animal Use Ethics

All work involving the use of live mice was done in compliance with the University of California, Riverside's Institutional Animal Care and Use Committee (IACUC) and National Institute of Health (NIH) guidelines. Male and female C57BL/6 mice were purchased from Jackson Labs (Sacramento, CA) at 8 weeks old. Mice were

acclimated for approximately one week in a specific-pathogen free vivarium (University of California, Riverside) before use in our chamber exposure studies.

Chamber Exposures

Cages of 3-4 C54BL/6 mice were randomized between control air and dust exposure treatment chambers (22) with access to food and water. Equal distribution of male and female mice were maintained between both chambers.

For the duration of each 7-day experiment, the control chamber was filled with dry, filtered air. In the dust exposure chamber, aqueous dust suspension was aerosolized with filtered air and passed through a silica drying column (23). The aerosolized filtrate was maintained at an average of 1500 $\mu g/m^3$ over the 7 days.

Mouse Lung & Fecal Dissection

At the end of each exposure period, mice were euthanized with isoflurane and cervical dislocation as per humane animal use protocols. The lower respiratory tract was extracted from below the mid-trachea, then floated and washed in 1x phosphate buffered saline (PBS) before the left and right lung lobes were separated at the tracheal bifurcation.

For a subset of experimental mouse cohorts (PD 2022, AG2022, and WI 2022), individual fecal pellet samples were collected directly from the large intestine. Lung and fecal samples were stored in their respective collection tubes at -80°C before microbial DNA extraction.

Flow Cytometry

Bronchoalveolar lavage fluid (BALF, 2.4mL) was collected from a subset of mice for digestion and staining for flow cytometry. Samples were stained with fluorescent antibodies: anti-CD45 FITC (BioLegend, San Diego, USA; Clone 30-F11), anti-CD19 PE-Cy5 (eBioscience, San Diego, USA; Clone MB19-1), anti-CD3 Alexa Fluor 700 (BioLegend, San Diego, USA; Clone 17A2), anti-Ly6G BV510 (BioLegend, San Diego, USA; Clone 1A8), anti-CD11b BV421 (BioLegend, San Diego, USA; Clone M1/70), anti-CD11c PE-Cy7 (BioLegend, San Diego, USA; Clone N418) and anti-SiglecF APC (BioLegend, San Diego, USA; Clone S17007L).

Flow cytometry was performed on a MoFlo Astrios (Beckman Coulter, Carlsbad, CA) and gating was done using FlowJo (Version 10.71). Raw cell count data was exported and analyzed in RStudio (R software version 3.18). The Shapiro-Wilks test was used to determine a non-normal distribution of neutrophil recruitment data among all BALF samples ($P<0.001$), so pairwise comparisons between contemporaneous control air and dust-exposure groups were performed with a Wilcoxon signed-rank test for non-normally distributed data.

Lung Microbiome Library Prep and Sequencing

Whole- or half-lung lobes were extracted using a modified protocol for the HostZERO Microbial DNA extraction kit (Zymo Research, Irvine, CA) for solid tissue samples (14). This modification included tissue lysis on an MP Bio Fastprep Classic (MP

Biomedicals, Irvine, CA) with 2.0mm beads. Microbial and eukaryotic components were separated by centrifugation, incubated with Proteinase K, and mechanically lysed and centrifuged before proceeding with the manufacturer's recommended protocol. Final sample yield was maximized by duplicating intermediate supernatant collections, which were combined as a single sample (per animal) at the end of the protocol. Negative controls were included in each DNA extraction and used in downstream analyses to control for contaminants. Samples were quantified with High Sensitivity Qubit (Invitrogen, Carlsbad, CA) and those with detectable concentrations of DNA were sent to Zymo Research (Irvine, CA) for 16S V3-V4 rRNA targeted-amplicon library preparation and gene sequencing.

Samples were treated with a PCR inhibitor removal step using the OneStep PCR Inhibitor Removal Kit (Zymo Research, Irvine, CA). Next, 16S rRNA V3-V4 amplification was done using the Quick-16S NGS Library Prep Kit (Zymo Research, Irvine, CA) with added mitochondrial-specific Peptide Nucleic Acid (mPNAs; mitochondrial blockers) clamps to minimize amplification of eukaryotic host mitochondrial DNA (24). Library sequencing was done on an Illumina NextSeq2000™ using the P1 reagent kit (600 cycles) and a 30% PhiX spike to promote read diversity.

Fecal Microbiome Library Prep and Sequencing

One fecal pellet per mouse was extracted for microbial DNA using the Qiagen PowerSoil Pro kit (Qiagen USA, Germanland, MD) as per manufacturer's protocols with exception to a bead beating and heated lysis step. Samples were homogenized in the bead

beater in 1 minute increments for 5 minutes total (MP Fastprep-24, MP Biomedicals, Irvine, CA) before an overnight heated lysis at 65ºC. After proceeding with the kit protocol, samples were eluted into 50uL of elution buffer.

DNA extracts were amplified using Klindworth 16s rRNA V3-V4 forward and reverse primers (25) and KAPA HiFi HotStart ReadyMix (Roche Molecular Systems Inc., U.S.A.). For amplification PCR, samples were denatured at 95ºC for 3 minutes, then 35 cycles were repeated for the following steps; 95ºC for 30 seconds, 55ºC for 30 seconds, 75ºC for 30 seconds. This was followed by a final extension at 72ºC for 5 minutes before samples were stored at 4ºC. PCR products were cleaned with AMPure XP beads (1:0.8 ratio, Beckman Coulter Life Sciences Inc., U.S.A.) before indexing.

Indexing was done using Illumina Nextera XT indexing primers (Illumina, San Diego, CA) and KAPA HiFi HotStart ReadyMix. The aforementioned thermal cycler settings were used with 8 cycles instead of 34. Indexed products were cleaned with AMPure XP beads (1:1). Products were quantified with a Qubit dsDNA High Sensitivity assay kit (Invitrogen, Carlsbad, CA) before pooling for sequencing. Amplicon sequencing was done with Illumina Miseq 2x300 paired end reads at University of California, Riverside's Genomics Core.

Bioinformatics– 16S rRNA Amplicon Sequence Analysis

All 16S rRNA (V3-V4) amplicon sequence data were analyzed respectively using a DADA2 workflow developed by Freund (12). Sequence quality was assessed using FastQC and eestats2 (26). Amplicon sequence variants (ASVs) were assigned in DADA2

using the Silva Database v138.2 (27). Negative controls were used to identify potential contaminants in their respective library and were removed using the R "decontam" package.

Statistical Analysis

All statistical analysis for 16S rRNA amplicon sequencing data were analyzed in RStudio (R software version 3.18). Taxa data from multiple Illumina MiSeq 16S rRNA amplicon sequencing runs were merged on a genus-species level before diversity analyses.

For alpha-diversity analyses, the Shapiro-Wilks test was used to determine distribution normality. For non-normal data, pairwise comparisons between contemporaneous exposure groups and among same-site dust-exposure groups were made using a Wilcoxon signed rank test. For normally distributed data, a two sample t-test was used. All P-values are reported after Bonferroni adjustment.

The R "vegan" package was used for beta diversity analyses. Species count data was transformed by center-log ratio (CLR, R "decostand") to generate an Aitchison distance matrix (28–30) and visualized in a Principal Coordinates Analysis (PCoA). Homogeneity of variance was analyzed using "betadisper" and permutational multivariate analysis of variance (PERMANOVA) was performed using "adonis2", followed by pairwise comparisons with "pairwiseAdonis" (31). All P-values are reported after Bonferroni adjustment.

Results

Lung Microbiome Composition and Dust Collection Season

We used a Principal Coordinate Analysis (PCoA) based on Aitchison distance matrices to visualize these compositional differences according to exposure material and colored by dust collection year (Fig. 2.2). An analysis of variance (ANOVA) test was used to determine significant differences in dispersion among exposure material groups and determined that spatial medians between groups were not significant ($P=0.2627$). It was found that lung microbiome composition significantly varied according to exposure material ($P=0.001$). Pairwise comparisons revealed that the lung microbiomes of control air-exposed mice significantly differed from WI 2022 ($P<0.01$), AG 2022 ($P<0.01$), and PD 2022 ($P<0.01$) dust-exposed mice. Similarly, lung microbiome composition of WI 2022 dust-exposed mice significantly differed from that of WI 2021 dust-exposed mice ($P<0.01$).

Lung Microbiome Diversity by Exposure Material

The core microbiome analysis by Lahti and Shetty (32) was used to visualize evenness and prevalence in mouse lung microbiomes according to exposure material. Prevalence was calculated for samples within each exposure material group based on a 1% genera relative abundance threshold and the top 25 genera across all samples were used to generate a heat map (Fig. 2.3), and an extended table of the top 100 genera has been included in the supplementary materials (Table S1). A Shapiro-Wilk's test determined that evenness was non-normally distributed ($P<0.001$), so a Kruskal-Wallis

test was used to reveal that Pielou's evenness significantly varied among groups according to exposure material (P=0.0026). Dunn's post-hoc test determined that lung microbiome evenness in WI 2020 dust-exposed mice was significantly higher than that of WI 2021 dust-exposed mice (P=0.0134) and WI 2022 dust-exposed mice (P=0.0316). A significant difference in evenness was also marginally observed between lung microbiomes of WI 2020 dust-exposed mice and AG 2022 dust-exposed mice (P=0.0479). Enrichment in gram-negative taxa with wide metabolic capacity and opportunistic associations with human pathogenicity were observed. This group included genera such as *Acinetobacter*, which was noticeably enriched in all 2022 dust-exposed groups and is clinically associated with pneumatic infection and natural disaster related disease outbreaks (33). *Staphylococcus*, a genus associated with lung microbiomes of healthy and diseased patients (34), was prevalent across sample groups but particularly enriched in WI 2021, WI 2022, AG 2022, and PD 2021 dust-exposed samples. The *Pseudomonas* genus was also more prevalent among all 2022 and WI 2020 dust-exposed groups, which has been observed in healthy clinical lavage samples (35), but is more commonly associated with lower airway inflammation and COPD. Patients with enriched *Pseudomonas* colonization have been shown to exhibit more frequent exacerbations and more severe disease symptoms (36–38).

We calculated Shannon-Wiener diversity and species richness for each treatment group. The Shapiro-Wilk's test found that both Shannon-Wiener diversity and species richness was non-normally distributed (Shannon-Wiener, P<0.001; species richness, P<0.001) so a Wilcoxon signed rank test was used to analyze pairwise differences in

means between contemporaneous treatment groups and same-site dust-exposure groups. For Shannon-Wiener diversity (Fig. 2.4), no contemporaneous pairs significantly differed from each other; however, lung microbiome diversity of mice exposed to WI 2021 dust significantly differed from that of mice exposed to WI 2020 dust (P=0.002) and WI 2022 dust (P=0.007). The lung microbiome diversity of mice exposed to WI 2020 dust also significantly differed from mice exposed to WI 2022 dust (P=0.002). For species richness (Fig. 2.5) lung microbiomes WI 2020 dust-exposed mice significantly differed from their contemporaneous control-air group (P=0.032). This was similarly observed among WI 2022 dust-exposed mice and their respective control group (P=0.009). Species richness in WI 2021 dust-exposed lungs significantly differed from WI 2022 dust-exposed lungs (P=0.005) and was marginally significant in comparison to WI 2020 dust-exposed lungs (P=0.045).

Fecal Microbiome Diversity and Composition After Dust Exposure

Variation in fecal microbiome composition was visualized in a PCoA using Aitchison distances and revealed distinct cohort biases among treatment groups (Supplementary Fig. S2.2). A PERMANOVA determined that this variance was significantly different (P=0.003), and a post-hoc test ('pairwiseAdonis') revealed a significant difference between fecal microbiome composition of WI 2022 dust-exposed mice and their contemporaneous controls (Fig. 2.6, P=0.015). No additional significant pairwise comparisons were observed between contemporaneous groups.

To minimize the influence of cohort-attributed biases between experimental groups, we used pairwise tests to compare Shannon-Diversity and species richness between dust exposure groups and their respective control-air group only. The Shapiro-Wilk test found that Shannon-Wiener diversity data was normally distributed across all samples (P=0.63) while species richness was non-normally distributed (P=0.03). A two-sample t-test found that Shannon-Wiener diversity significantly differed in fecal microbiomes of WI 2022 dust-exposed mice when compared to their contemporaneous controls (Fig. 2.7A, P=0.021). Similarly, a Wilcoxon signed rank test determined that species richness significantly differed in fecal microbiomes of WI 2022 dust-exposed mice when compared to their contemporaneous controls (Fig. 2.7B, P=0.013). In contrast, Shannon-Wiener diversity and species richness was not significantly different for fecal microbiomes of PD 2022 dust- or AG 2022 dust-exposed mice and their contemporaneous controls.

Host Inflammation in Response to Salton Sea Dust Exposure

Host neutrophil recruitment was calculated as a proportion of CD54+ lymphocytes (Fig. 2.8). The Wilcoxon signed rank test was used for pairwise comparisons between each dust-exposed group and their contemporaneous control air-exposed group. All pairwise comparisons were found to be equally significant according to the signed rank test (P=0.03), with exception to WI 2021 dust-exposed mice and their respective control group (P=0.06), and AG 2022 dust-exposed mice and their respective control group (P=0.30). A box plot was used to visualize neutrophil recruitment among

treatment groups and revealed that WI 2020 and WI 2022 dust-exposed mice experienced a greater magnitude of neutrophilic pulmonary inflammation in comparison to other treatment groups, despite the statistical pairwise comparisons. Additionally, exposure to AG 2021 dust appeared to elicit a heighted neutrophilic response but at a lower degree than Wister groups.

Compositional Variation Between Lung and Fecal Microbiomes

Lung and fecal microbiome data from PD 2022, AG 2022, and WI 2022 exposures were merged and compositional differences based on chamber (Control vs. Dust) and sample type (Fecal vs. Lung) were visualized in a PCoA using an Aitchison distance matrix (Fig. 2.9). It was revealed that the lung and fecal microbiomes remained distinct from each other; this distinction was confirmed via PERMANOVA, which determined significant differences in variation between microbiome composition according to chamber and sample type (P=0.003).

Discussion

This chapter examined the extent of spatiotemporal dust variation on the murine lung microbiome following chronic 7-day exposure. Additionally, we assessed changes in host pulmonary inflammation and the fecal microbiome to contextualize shifts in the lung microbiome within a greater systemic response.

It was expected that spatiotemporal variation in environmental dust would differentially affect lung microbiome composition and diversity. We found that exposure

to abiotic dust filtrate collected at the Salton Sea in the summer-early fall of 2022 led to significant shifts in lung microbiome composition when compared to control air-exposed mice (Fig. 2.2). Previous work from our group examined the effects of seasonal variation on the Salton Sea dust microbiome, and found that precipitation, surface type frequency, and average wind speeds were the primary drivers for compositional differences in the aeolian microbiome between 2020 and 2021 (13). Similar studies have found that temperature variation and nutrient availability significantly alter atmospheric bacteriomes across seasons, and its interaction with the atmospheric mycobiome – which is independently manipulated by seasonal weather events – is predictive of total aeolian community composition and function (5). Environmental variables that ultimately affect aeolian microbiome composition may indirectly affect that of the lung microbiome, assuming the lung microbiome directly reacts to biochemical compositions of environmental aerosols. Studies taking place in Denver, Colorado and across various districts within China's Fujian province note that fungi and potential pathogens are more enriched in the dust microbiome during warmer spring and summer months (5,39) which in turn, may correlate with enriched microbial byproducts such as spores and endotoxins present in the local air space. LPS (lipopolysaccharide), an endotoxin originating from the cell membrane of gram- negative bacteria, has been understood to remain on previously contaminated cigarette surfaces, indirectly exacerbating pulmonary inflammation among smokers (40,41). This demonstrates that the presence of viable, intact bacterial cells is not necessary for inducing a neutrophilic pulmonary response via exposure. Further, LPS's capacity to persist in the environment implies that microbial

enrichment from season to season may favor the buildup of such byproducts rather than decay.

While it is expected that neutrophil recruitment in the lung would be inversely correlated with microbial richness because the greater number of neutrophils, the lower the survival of microorganisms, our finding suggest that is not the case among dust-exposed mice. In fact, we found a positive correlation among microbial parameters and heightened neutrophil recruitment (Fig. 2.8); this recruitment was observed alongside increased Shannon-Wiener diversity (Fig. 2.4), species richness (Fig. 2.5), as well as decreased evenness (Fig. 2.3), which suggests that more neutrophils may relate to more microbes; however, not all microorganisms increase along with heightened neutrophil recruitment. This is consistent with findings in Chapter 1, suggesting greater complexity in the host inflammation and lung microbiome relationship.

The nature of our methods assume that no viable bacterial cells were aerosolized in these chamber experiments, and we did not directly seed the lung microbiome through exposure; thus, the shifts in lung microbiome composition and diversity among dust-exposed lungs are more likely shifts occurring within a pre-existing community. Increased diversity and richness, and decreased evenness alongside heightened neutrophil recruitment suggests that the host immune system is disproportionately responding to bacterial signals rather than the bacterial cells themselves, lending an opportunity for particular taxa to proliferate. A previous study demonstrated that acute lung injury simulated by intratracheal injection of sterile LPS resulted in neutrophil domination in BALF samples, along with a significant shift in lung microbiome composition; however,

these microbiomes displayed insignificant changes in diversity after injection (42). Thus, the volume or route of LPS introduction in the airway may differentially impact lung microbiome composition and diversity. Further, studies looking at the lung microbiome during pulmonary disease states, increased bacterial diversity was typical of asthma patients, while decreased diversity and evenness was associated with COPD patients (34,36,38,43), demonstrating that the lung microbiomes in this study do not directly comply with any one disease phenotype, highlighting the unique and variable consequences of environmental-based exposures on pulmonary health and the microbiome.

Mouse fecal microbiomes were examined alongside their respective lung microbiomes to determine if the effects of dust exposure could be observed in a distal microbiome, which does not directly interface with the dust. Previous research has pointed at the influence of environmental variables on the gut microbiome, particularly in the context of climate-related ecological shifts, public health burdens, and seasonal weather events (18,44,45). Broadly, psychosocial stress – which can be triggered by environmental input – is consistently associated with gut microbiome dysbiosis, characterized by reduced diversity and compositional shifts (46,47). We expected that shifts in the fecal microbiome would be observed if chronic dust exposure and subsequent pulmonary inflammation had greater systemic stress effects on the host. Overall, fecal microbiome composition across exposure groups separated according to cohort biases; however, pairwise comparisons found composition (Fig. 2.6), Shannon-Wiener diversity, and richness (Fig. 2.7) in fecal microbiomes of WI 2022 dust-exposed

mice to be significantly different from their contemporaneous controls. In comparison to the lung microbiomes of WI 2022 dust-exposed mice in which significant increases in diversity (Fig. 2.4) and richness (Fig. 2.5) were observed the opposite was true in fecal microbiomes. Direct depletion of the gut microbiome has been previously associated with adverse health effects, as antibiotic-treated and germ-free mice were shown to exhibit higher susceptibility to viral and bacterial respiratory infection. Further, the gut microbiome's role in regulating systemic inflammatory responses have pointed to the 'gut-lung axis' as a critical player in modulating COPD exacerbations and asthma by way of inflammatory mediators and ligand signaling through circulation or mucosa (15,17,35). This significant depletion of fecal microbiome diversity therefore suggests that chronic exposure to Salton Sea dust acts as a systemic stressor, reflected by the magnitude of pulmonary neutrophil recruitment observed in WI 2022 dust-exposed mice (Fig. 2.8).

While the effects of Salton Sea dust exposure have been consistently associated with local acute neutrophilic inflammation in the lung (14,21), this study begins to examine the holistic effects of chronic inflammatory dust exposure, specifically across the host microbiome. Our findings determined that spatiotemporal variation in the dust has differential impacts on lung microbiome composition and diversity. It can be speculated that site-by-seasonal differences in the environmental dust microbiome– mediated by local wind patterns, temperature, and precipitation– enrich the aerosols with microbial byproducts or biochemical triggers which elicit the characteristic neutrophilic response we've observed across experiments. The consequences may trigger systemic

stress in exposed hosts, which generally result in significant increases in diversity among the lung microbiome, and significant decrease in diversity in the gut microbiome.

Although it may be difficult to thoroughly elucidate the detrimental implications on public health, in the Salton Sea basin, we have begun to unravel the consequences of a desiccating lakebed on the environment and health within the context of a shifting host-microbiome. As rapid industrialization and environmental negligence exacerbate aerosol pollutants in proximal communities, it will be pertinent to consider the cascading consequences ranging from ecological consideration to mounting threats to human health and safety.

List of Figures

sample t-test and revealed fecal diversity in WI 2022 dust-exposed mice to be significantly lower than their respective control air-exposed group (P=0.021). **(B)** Species richness was similarly compared using a Wilcoxon signed rank test and revealed fecal species richness in WI 2022 dust-exposed was significantly lower than their control air exposed group (P=0.013).

Fig 2.9 Lung neutrophil recruitment by treatment group. Neutrophil recruitment was analyzed as a proportion of CD45+ lymphocytes and pairwise comparisons were made between contemporaneous groups using a Wilcoxon signed rank test. Stars (*) indicate a significant pairwise comparison between a dust exposure group and its contemporaneous control (P<0.03). All pairs were significant with exception to the AG 2022 and WI 2021 exposures.

Fig 2.10 Comparing composition of mouse lung and fecal microbiomes. A principal coordinates analysis (PCoA) was used to visualize the composition of lung and fecal microbiomes, which were significantly distinct from each other, regardless of dust or control air treatment (PERMANOVA, P=0.003).

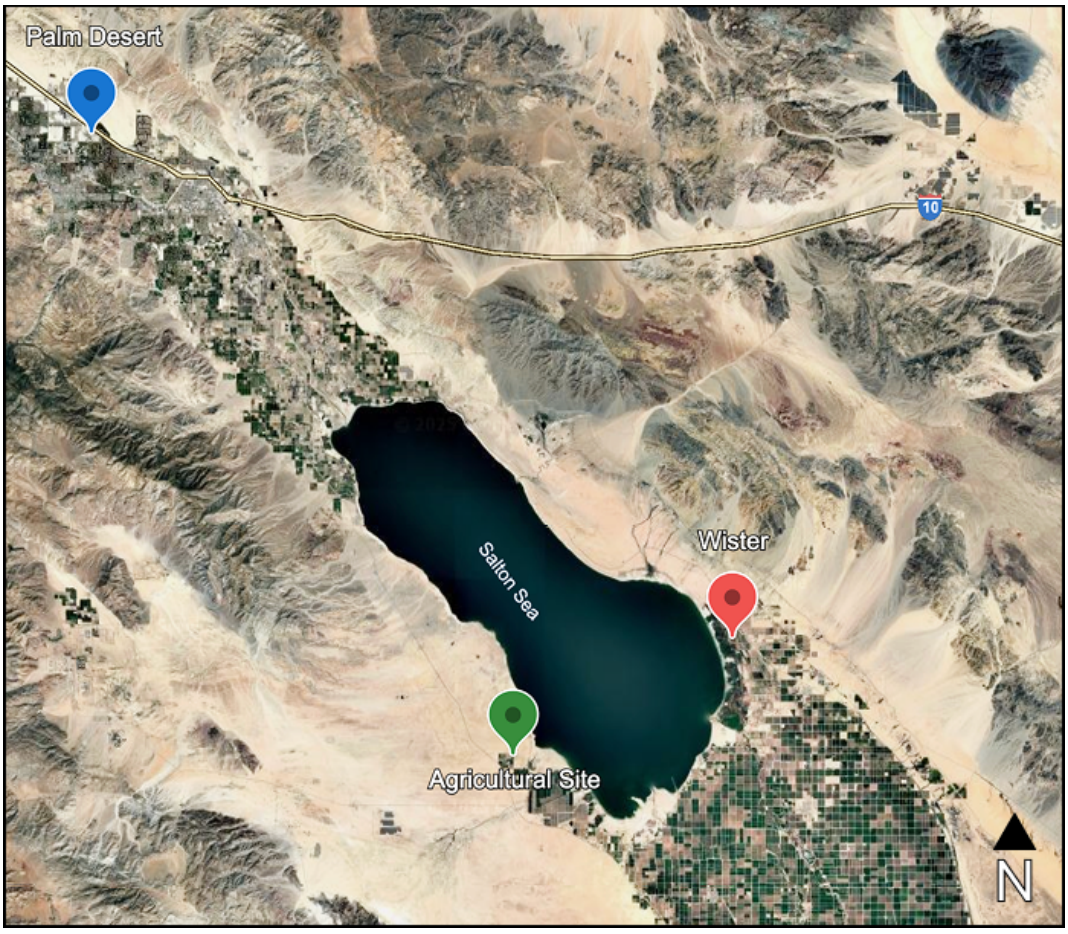

Figure 2.2 Map of the Salton Sea including markers for each dust collection site. Palm Desert (PD, blue) is located approximately 26 miles from the Salton Sea perimeter. Wister (WI, red) and Agricultural site (AG, green) are located <2 miles from the Salton Sea perimeter.

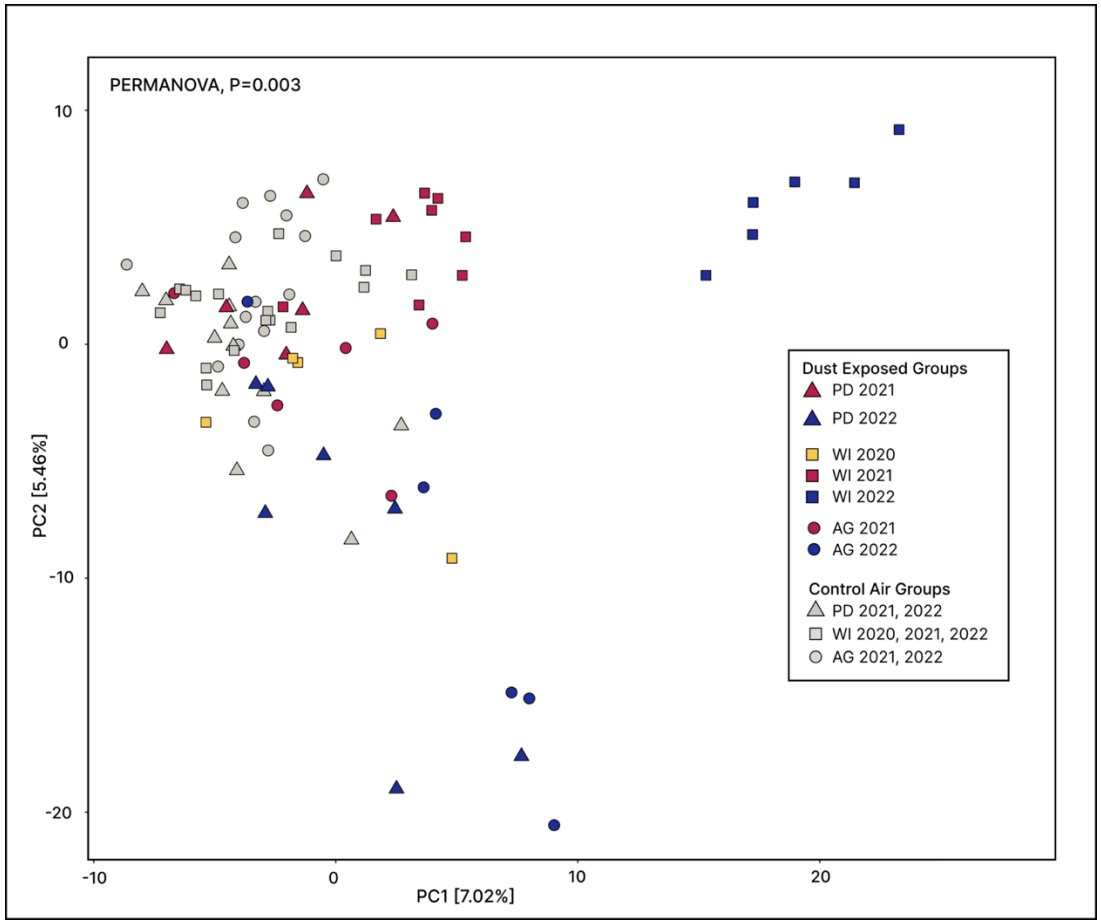

Figure 2.3 Lung microbiome beta-diversity. Principal coordinates analysis (PCoA) on mouse lung microbiomes using center-log ratio transformed distances (CLR Aitchison). Points are shaped according to dust collection site and colored by dust collection year. Variation between exposure material groups was found to be significantly different (PERMANOVA, P=0.003).

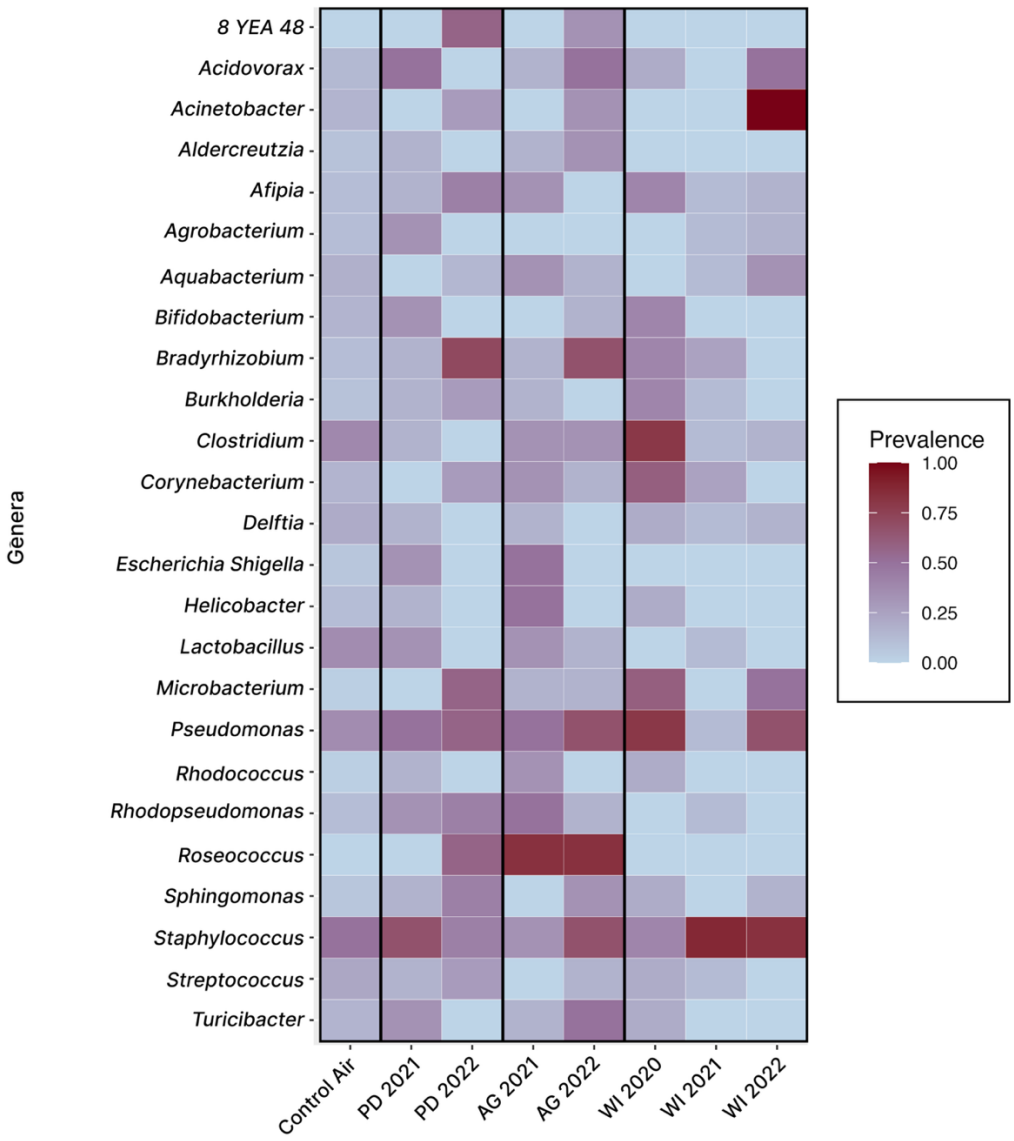

Figure 2.4 Top 25 genera prevalence by exposure material. Heatmap depicting prevalence (presence in samples at 1% relative abundance) highlights variation in evenness among samples according to exposure material.

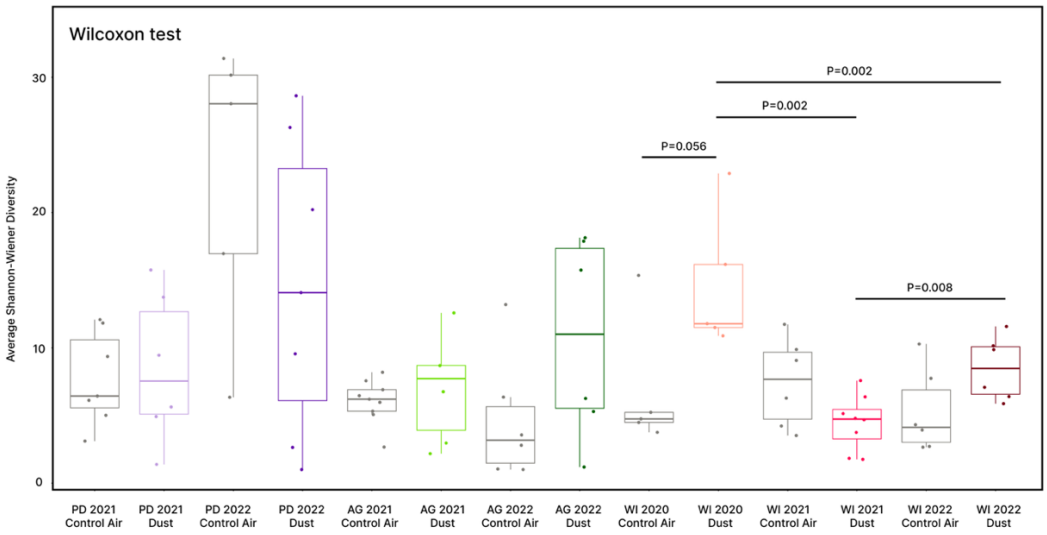

Figure 2.5 Lung microbiome Shannon-Wiener diversity. Average Shannon-Wiener diversity indexes were plotted according to treatment group and a Wilcoxon test was used to determine significant differences between contemporaneous or same-site pairs. Lung microbiome diversity in WI 2020 dust-exposed mice was significantly different from that of WI 2021 dust-exposed mice (P=0.002) and WI 2022 dust-exposed mice (P=0.002). Lung microbiome diversity in WI 2021 dust-exposed mice were also significantly different from WI 2022 dust-exposed mice (P=0.008).

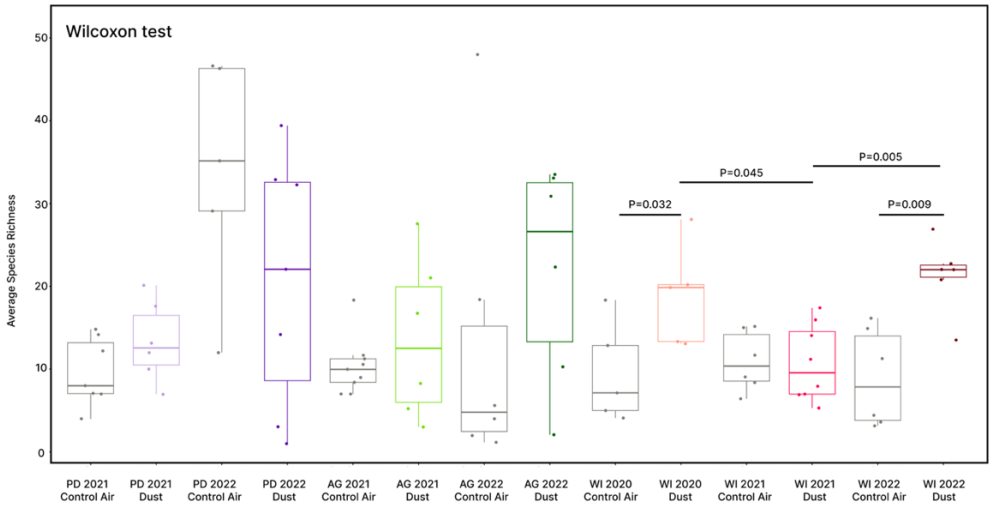

Figure 2.6 Lung microbiome species richness. Average species richness was plotted according to treatment group and a Wilcoxon test was used to determine significant differences between contemporaneous or same-site pairs. In comparison to their contemporaneous control air-exposed groups, lung microbiome richness significantly differed in WI 2020 dust-exposed mice (P=0.032) and WI 2022 dust-exposed mice (P=0.009). Lung microbiome richness in WI 2021 dust-exposed mice significantly differed from WI 2020 dust-exposed mice (P=0.045) and WI 2022 dust-exposed mice (P=0.009).

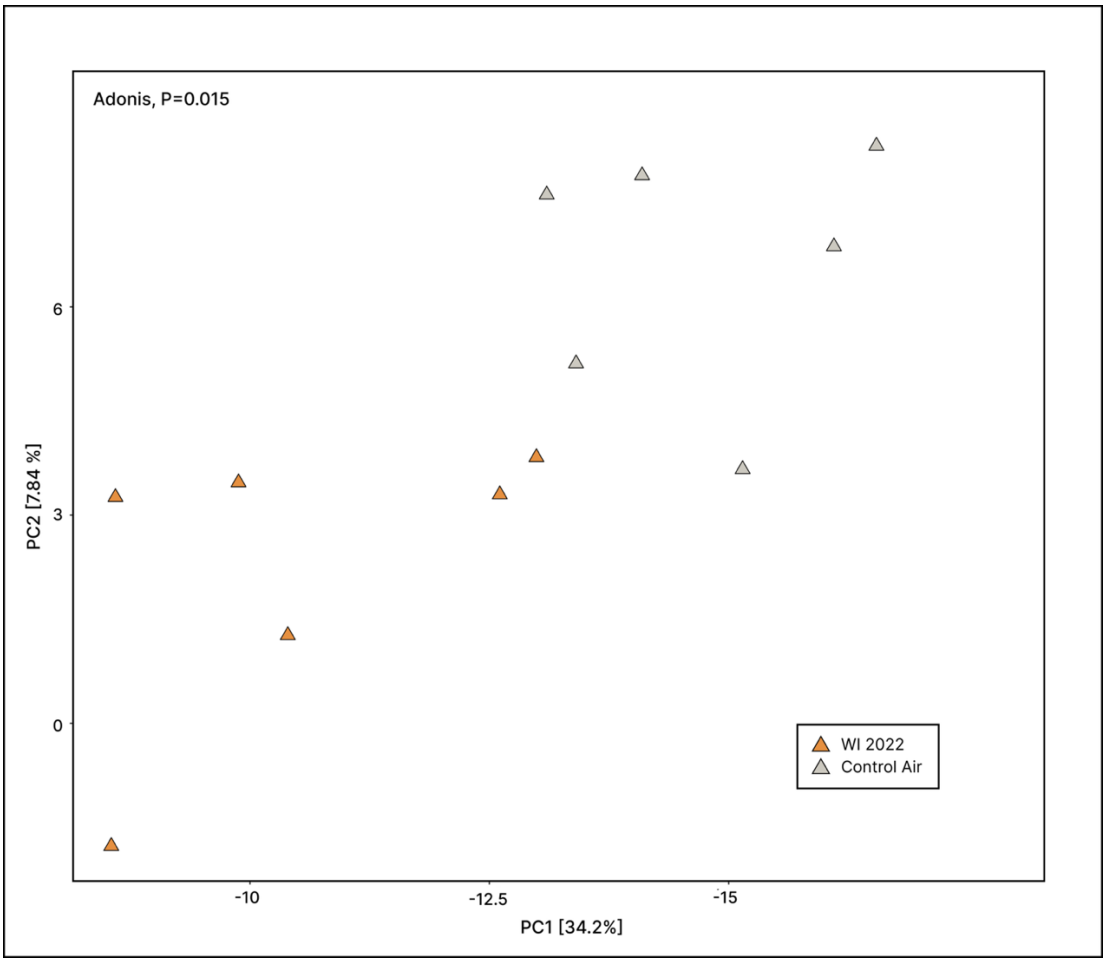

Figure 2.7 Fecal microbiome composition in WI 2022 dust-exposed mice. A principal coordinate analysis (PCoA) using center-log ratio (CLR, Aitchison) distances revealed dissimilarities in fecal microbiome composition for WI 2022 dust-exposed mice and their contemporaneous controls. Pairwise adonis revealed this difference to be significant (P=0.015).

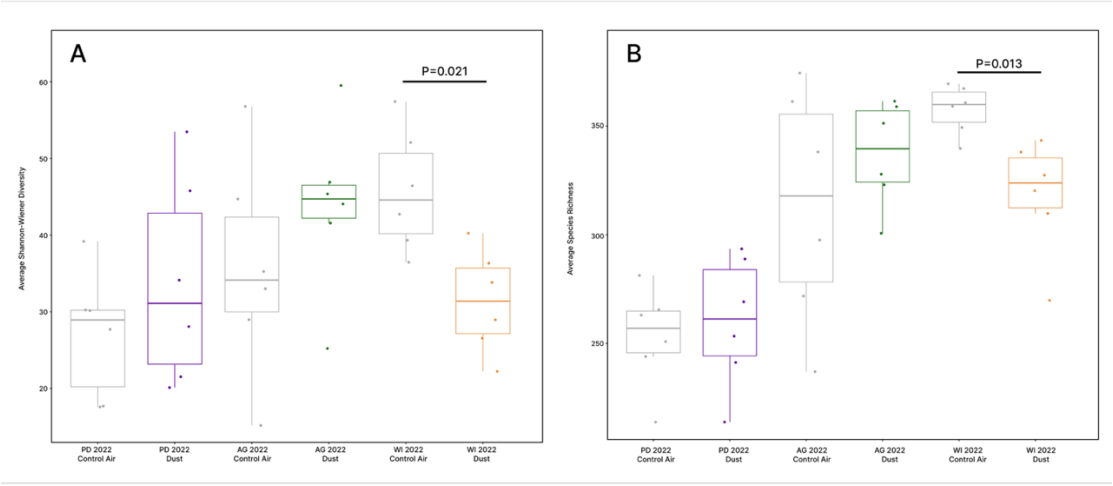

Figure 2.8 Mouse fecal microbiome diversity according to treatment group. (A) Shannon-Wiener diversity was compared between contemporaneous pairs using a two-sample t-test and revealed fecal diversity in WI 2022 dust-exposed mice to be significantly lower than their respective control air-exposed group (P=0.021). **(B)** Species richness was similarly compared using a Wilcoxon signed rank test and revealed fecal species richness in WI 2022 dust-exposed was significantly lower than their control air exposed group (P=0.013).

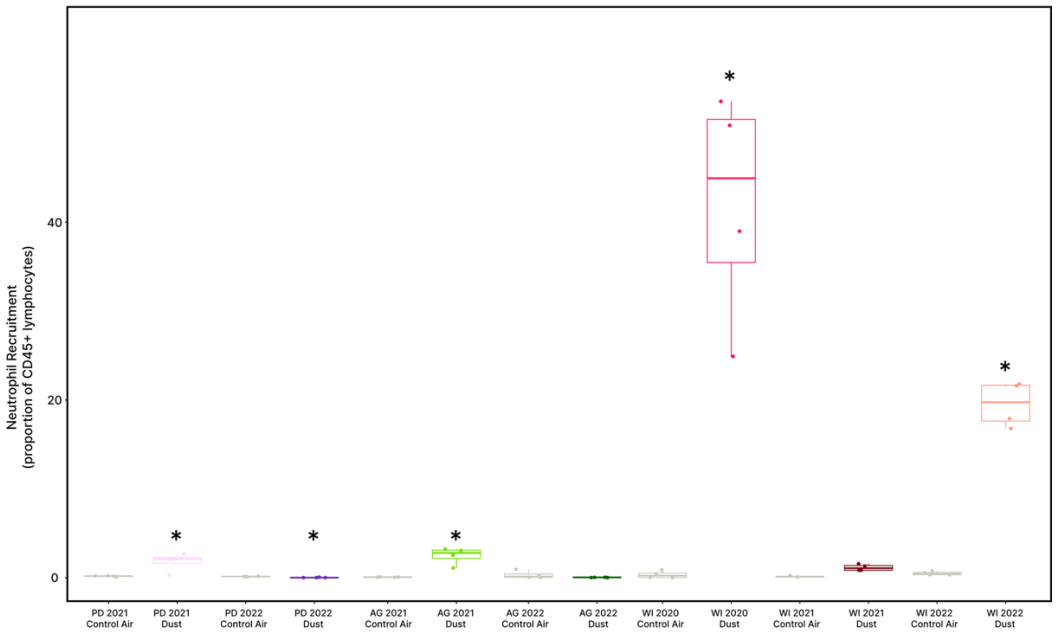

Figure 2.9 Lung neutrophil recruitment by treatment group. Neutrophil recruitment was analyzed as a proportion of CD45+ lymphocytes and pairwise comparisons were made between contemporaneous groups using a Wilcoxon signed rank test. Stars (*) indicate a significant pairwise comparison between a dust exposure group and its contemporaneous control ($P<0.03$). All pairs were significant with exception to the AG 2022 and WI 2021 exposures.

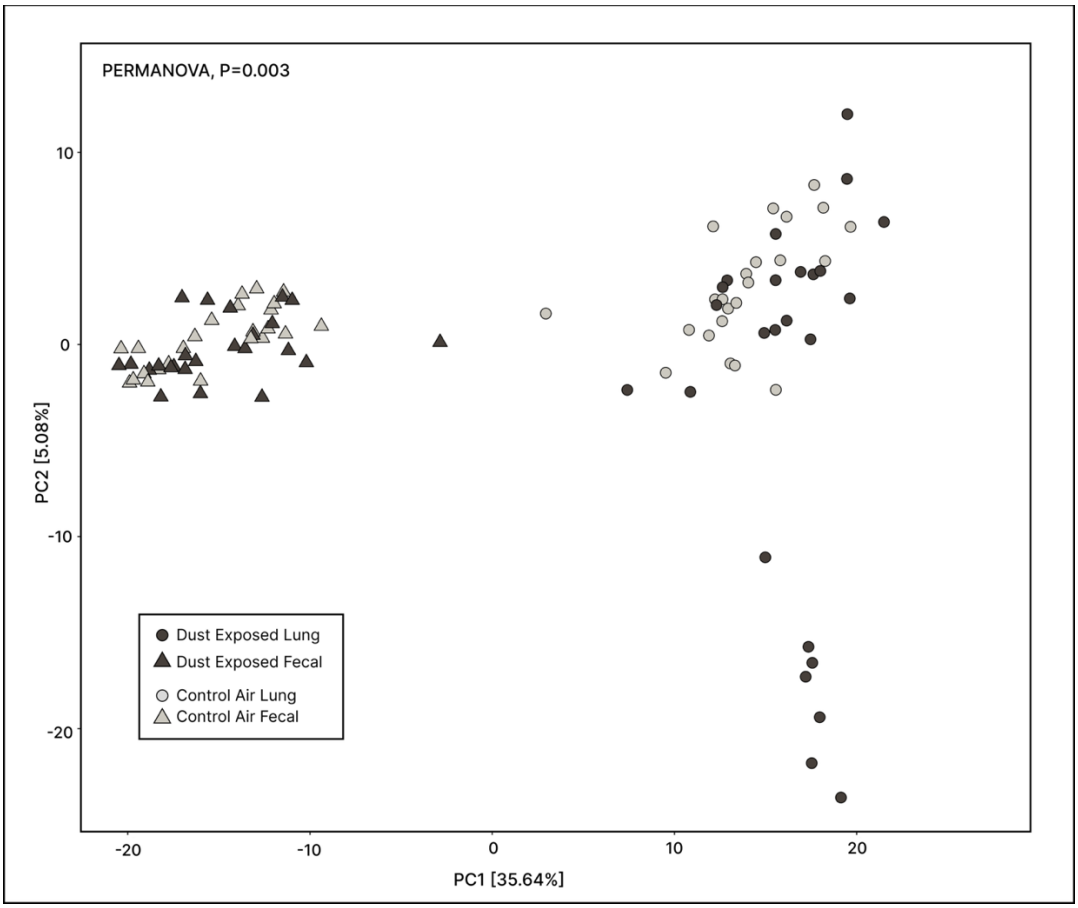

Figure 2.10 Comparing composition of mouse lung and fecal microbiomes. A principal coordinates analysis (PCoA) was used to visualize the composition of lung and fecal microbiomes, which were significantly distinct from each other, regardless of dust or control air treatment (PERMANOVA, P=0.003).

References

1. Gilbert JA, Stephens B. Microbiology of the built environment. Nat Rev Microbiol. 2018 Nov;16(11):661–70.

2. Johnston JE, Razafy M, Lugo H, Olmedo L, Farzan SF. The disappearing Salton Sea: A critical reflection on the emerging environmental threat of disappearing saline lakes and potential impacts on children's health. Sci Total Environ. 2019 May;663:804–17.

3. Jones BA, Fleck J. Shrinking lakes, air pollution, and human health: Evidence from California's Salton Sea. Sci Total Environ. 2020 Apr;712:136490.

4. Calderón-Ezquerro MDC, Serrano-Silva N, Brunner-Mendoza C. Aerobiological study of bacterial and fungal community composition in the atmosphere of Mexico City throughout an annual cycle. Environ Pollut. 2021 Jun;278:116858.

5. Li H, Liu PQ, Luo QP, Ma JJ, Yang XR, Yan Y, et al. Spatiotemporal variations of microbial assembly, interaction, and potential risk in urban dust. Environ Int. 2022 Dec;170:107577.

6. Maltz MR, Carey CJ, Freund HL, Botthoff JK, Hart SC, Stajich JE, et al. Landscape Topography and Regional Drought Alters Dust Microbiomes in the Sierra Nevada of California. Front Microbiol. 2022 Jun 28;13:856454.

7. Freund H, Maltz MR, Swenson MP, Topacio TM, Montellano VA, Porter W, et al. Microbiome interactions and their ecological implications at the Salton Sea. Calif Agric. 2022 Apr;76(1):16–26.

8. Vogl RA, Henry RN. Characteristics and contaminants of the Salton Sea sediments. In: Barnum DA, Elder JF, Stephens D, Friend M, editors. The Salton Sea [Internet]. Dordrecht: Springer Netherlands; 2002 [cited 2025 Jun 5]. p. 47–54. Available from: http://link.springer.com/10.1007/978-94-017-3459-2_3

9. Frie AL, Dingle JH, Ying SC, Bahreini R. The Effect of a Receding Saline Lake (The Salton Sea) on Airborne Particulate Matter Composition. Environ Sci Technol. 2017 Aug 1;51(15):8283–92.

10. Cohen MJ, Morrison JI, Glenn EP. The Ecology and Future of the Salton Sea.

11. Hung C, Diamond C, Sinclair R, Lee MC, Stenstrom M, Freilich MA, et al. Nutrient loading as a key cause of short- and long-term anthropogenic ecological degradation of the Salton Sea. Sci Rep. 2024 Dec 28;14(1):31247.

12. Freund L, Hung C, Topacio TM, Diamond C, Fresquez A, Lyons TW, et al. Diversity of sulfur cycling halophiles within the Salton Sea, California's largest lake. BMC Microbiol. 2025 Mar 6;25(1):120.

13. Freund L. The Microbial Ecology of the Salton Sea: How an Extreme Environment Selects for Microbial Metabolism & Survival. [Riverside, CA]: University of California, Riverside; 2024.

14. Maltz MR, Topacio T, Lo DD, Freund L, Zaza M, Botthoff JK, et al. Lung microbiomes' variable responses to dust exposure [Internet]. Molecular Biology; 2025 [cited 2025 Jul 1]. Available from: http://biorxiv.org/lookup/doi/10.1101/2025.04.10.648223

15. Wypych TP, Wickramasinghe LC, Marsland BJ. The influence of the microbiome on respiratory health. Nat Immunol. 2019 Oct;20(10):1279–90.

16. Perdijk O, Azzoni R, Marsland BJ. The microbiome: an integral player in immune homeostasis and inflammation in the respiratory tract. Physiol Rev. 2024 Apr 1;104(2):835–79.

17. McAleer JP, Kolls JK. Contributions of the intestinal microbiome in lung immunity. Eur J Immunol. 2018 Jan;48(1):39–49.

18. Litchman E. Climate change effects on the human gut microbiome: complex mechanisms and global inequities. Lancet Planet Health. 2025 Feb;9(2):e134–44.

19. Aciego SM, Riebe CS, Hart SC, Blakowski MA, Carey CJ, Aarons SM, et al. Dust outpaces bedrock in nutrient supply to montane forest ecosystems. Nat Commun. 2017 Mar 28;8(1):14800.

20. Maltz MR, Topacio T, Lo DD, Freund L, Zaza M, Botthoff JK, et al. Lung microbiomes' variable responses to dust exposure [Internet]. Molecular Biology; 2025 [cited 2025 Jul 1]. Available from: http://biorxiv.org/lookup/doi/10.1101/2025.04.10.648223

21. Biddle TA, Yisrael K, Drover R, Li Q, Maltz MR, Topacio TM, et al. Aerosolized aqueous dust extracts collected near a drying lake trigger acute neutrophilic pulmonary inflammation reminiscent of microbial innate immune ligands. Sci Total Environ. 2023 Feb;858:159882.

22. Peng X, Maltz MR, Botthoff JK, Aronson EL, Nordgren TM, Lo DD, et al. Establishment and characterization of a multi-purpose large animal exposure chamber for investigating health effects. Rev Sci Instrum. 2019 Mar 1;90(3):035115.

23. Biddle TA, Li Q, Maltz MR, Tandel PN, Chakraborty R, Yisrael K, et al. Salton Sea aerosol exposure in mice induces a pulmonary response distinct from allergic inflammation. Sci Total Environ. 2021 Oct;792:148450.

24. Lundberg DS, Yourstone S, Mieczkowski P, Jones CD, Dangl JL. Practical innovations for high-throughput amplicon sequencing. Nat Methods. 2013 Oct;10(10):999–1002.

25. Klindworth A, Pruesse E, Schweer T, Peplies J, Quast C, Horn M, et al. Evaluation of general 16S ribosomal RNA gene PCR primers for classical and next-generation sequencing-based diversity studies. Nucleic Acids Res. 2013 Jan 1;41(1):e1–e1.

26. Andrews S. Andrews S. FastQC: A Quality Control Tool for High Throughput Sequence Data. 2010. [Internet]. 2010. Available from: https://www.bioinformatics.babraham.ac.uk/projects/fastqc/

27. Quast C, Pruesse E, Yilmaz P, Gerken J, Schweer T, Yarza P, et al. The SILVA ribosomal RNA gene database project: improved data processing and web-based tools. Nucleic Acids Res. 2012 Nov 27;41(D1):D590–6.

28. Lubbe S, Filzmoser P, Templ M. Comparison of zero replacement strategies for compositional data with large numbers of zeros. Chemom Intell Lab Syst. 2021 Mar;210:104248.

29. Quinn TP, Erb I, Richardson MF, Crowley TM. Understanding sequencing data as compositions: an outlook and review. Wren J, editor. Bioinformatics. 2018 Aug 15;34(16):2870–8.

30. Quinn TP, Erb I, Gloor G, Notredame C, Richardson MF, Crowley TM. A field guide for the compositional analysis of any-omics data. GigaScience. 2019 Sep 1;8(9):giz107.

31. Martinez Arbizu P. pairwiseAdonis [Internet]. 2020. Available from: https://github.com/pmartinezarbizu/pairwiseAdonis

32. Lahti L, Shetty S. Core microbiome [Internet]. 2018. Available from: https://microbiome.github.io/tutorials/Core.html

33. Munoz-Price LS, Weinstein RA. Acinetobacter Infection. N Engl J Med. 2008 Mar 20;358(12):1271–81.

34. Marimón JM. The Lung Microbiome in Health and Respiratory Diseases. Clin Pulm Med. 2018 Jul;25(4):131–7.

35. He Y, Wen Q, Yao F, Xu D, Huang Y, Wang J. Gut–lung axis: The microbial contributions and clinical implications. Crit Rev Microbiol. 2017 Jan 2;43(1):81–95.

36. Kostric M, Milger K, Krauss-Etschmann S, Engel M, Vestergaard G, Schloter M, et al. Development of a Stable Lung Microbiome in Healthy Neonatal Mice. Microb Ecol. 2018 Feb;75(2):529–42.

37. Natalini JG, Singh S, Segal LN. The dynamic lung microbiome in health and disease. Nat Rev Microbiol. 2023 Apr;21(4):222–35.

38. Erb-Downward JR, Thompson DL, Han MK, Freeman CM, McCloskey L, Schmidt LA, et al. Analysis of the Lung Microbiome in the "Healthy" Smoker and in COPD. Bereswill S, editor. PLoS ONE. 2011 Feb 22;6(2):e16384.

39. Bowers RM, Clements N, Emerson JB, Wiedinmyer C, Hannigan MP, Fierer N. Seasonal Variability in Bacterial and Fungal Diversity of the Near-Surface Atmosphere. Environ Sci Technol. 2013 Nov 5;47(21):12097–106.

40. Hasday JD, Bascom R, Costa JJ, Fitzgerald T, Dubin W. Bacterial Endotoxin Is an Active Component of Cigarette Smoke. Chest. 1999 Mar;115(3):829–35.

41. Liu X, Sun W, Ma W, Wang H, Xu K, Zhao L, et al. Smoking related environmental microbes affecting the pulmonary microbiome in Chinese population. Sci Total Environ. 2022 Jul;829:154652.

42. Poroyko V, Meng F, Meliton A, Afonyushkin T, Ulanov A, Semenyuk E, et al. Alterations of lung microbiota in a mouse model of LPS-induced lung injury. Am J Physiol-Lung Cell Mol Physiol. 2015 Jul 1;309(1):L76–83.

43. Whiteside SA, McGinniss JE, Collman RG. The lung microbiome: progress and promise. J Clin Invest. 2021 Aug 2;131(15):e150473.

44. Davenport ER, Mizrahi-Man O, Michelini K, Barreiro LB, Ober C, Gilad Y. Seasonal Variation in Human Gut Microbiome Composition. Quintana-Murci L, editor. PLoS ONE. 2014 Mar 11;9(3):e90731.

45. Chakrabarti SK, Chattopadhyay D. Understanding The Eco-Gut Link: How Climate Shapes Gut Microbiome and Human Health. J Community Med Public Health Rep [Internet]. 2024 Aug 29 [cited 2025 Jun 5]; Available from: https://www.acquaintpublications.com/article/understanding_the_eco_gut_link_how_climate_shapes_gut_microbiome_and_human_health

46. Marwaha K, Cain R, Asmis K, Czaplinski K, Holland N, Mayer DCG, et al. Exploring the complex relationship between psychosocial stress and the gut

microbiome: implications for inflammation and immune modulation. J Appl Physiol. 2025 Feb 1;138(2):518–35.

47. Bidell MR, Hobbs ALV, Lodise TP. Gut microbiome health and dysbiosis: A clinical primer. Pharmacother J Hum Pharmacol Drug Ther. 2022 Nov;42(11):849–57.

Supplementary Materials

Table S2.1 Top 100 Genera prevalence (1% RA) in lung microbiomes by exposure material and sorted by highest to lowest mean prevalence

Fig S2.2 PCoA of fecal microbiome composition by treatment group using CLR-transformed (Aitchison) distances

Table S2.1 Top 100 Genera prevalence (1% RA) in lung microbiomes by exposure material and sorted by highest to lowest mean prevalence

Genus	Control Air	PD 2021	PD 2022	AG 2021	AG 2022	WI 2020	WI 2021	WI 2022	Mean prevalence
Pseudomonas	0.364	0.500	0.571	0.500	0.667	0.800	0.125	0.667	0.484
Staphylococcus	0.500	0.667	0.429	0.333	0.667	0.400	0.875	0.833	0.482
Roseococcus	0.000	0.000	0.571	0.833	0.833	0.000	0.000	0.000	0.351
Rhodopseudomonas	0.114	0.333	0.429	0.500	0.167	0.000	0.125	0.000	0.344
Bradyrhizobium	0.114	0.167	0.714	0.167	0.667	0.400	0.250	0.000	0.290
Afipia	0.114	0.167	0.429	0.333	0.000	0.400	0.125	0.167	0.261
Lactobacillus	0.364	0.333	0.000	0.333	0.167	0.000	0.125	0.000	0.258
Escherichia Shigella	0.068	0.333	0.000	0.500	0.000	0.000	0.000	0.000	0.225
Clostridium	0.386	0.167	0.000	0.333	0.333	0.800	0.125	0.167	0.222
Acidovorax	0.136	0.500	0.000	0.167	0.500	0.200	0.000	0.500	0.201
Helicobacter	0.114	0.167	0.000	0.500	0.000	0.200	0.000	0.000	0.195
Corynebacterium	0.159	0.000	0.286	0.333	0.167	0.600	0.250	0.000	0.195
Microbacterium	0.023	0.000	0.571	0.167	0.167	0.600	0.000	0.500	0.190
Burkholderia Caballeronia Paraburkholderia	0.091	0.167	0.286	0.167	0.000	0.400	0.125	0.000	0.177
Streptococcus	0.227	0.167	0.286	0.000	0.167	0.200	0.125	0.000	0.170
Sphingomonas	0.068	0.167	0.429	0.000	0.333	0.200	0.000	0.167	0.166
Turicibacter	0.159	0.333	0.000	0.167	0.500	0.200	0.000	0.000	0.165
Aquabacterium	0.182	0.000	0.143	0.333	0.167	0.000	0.125	0.333	0.165
8 YEA 48	0.000	0.000	0.571	0.000	0.333	0.000	0.000	0.000	0.143
Delftia	0.205	0.167	0.000	0.167	0.000	0.200	0.125	0.167	0.134
Rhodococcus	0.023	0.167	0.000	0.333	0.000	0.200	0.000	0.000	0.131
Bifidobacterium	0.159	0.333	0.000	0.000	0.167	0.400	0.000	0.000	0.123
Agrobacterium	0.114	0.333	0.000	0.000	0.000	0.000	0.125	0.167	0.112
Acinetobacter	0.159	0.000	0.286	0.000	0.333	0.000	0.000	1.000	0.111
Adlercreutzia	0.091	0.167	0.000	0.167	0.333	0.000	0.000	0.000	0.106
Enterococcus	0.114	0.167	0.143	0.000	0.167	0.200	0.000	0.000	0.106
Brevundimonas	0.068	0.333	0.000	0.000	0.000	0.000	0.000	0.167	0.100
Roseateles	0.091	0.000	0.143	0.167	0.000	0.000	0.000	0.167	0.100
Dubosiella	0.045	0.333	0.000	0.000	0.333	0.000	0.000	0.000	0.095
Atopostipes	0.091	0.000	0.286	0.000	0.167	0.600	0.000	0.000	0.094
Anaerococcus	0.045	0.000	0.143	0.167	0.000	0.000	0.000	0.000	0.089
Massilia	0.045	0.167	0.143	0.000	0.000	0.000	0.000	0.333	0.089

Mycobacterium	0.068	0.000	0.286	0.000	0.000	0.000	0.000	0.000	0.088
Rothia	0.068	0.000	0.286	0.000	0.000	0.200	0.000	0.000	0.088
Aminobacter	0.000	0.000	0.000	0.333	0.333	0.000	0.250	0.000	0.083
Paenarthrobacter	0.000	0.000	0.000	0.333	0.833	0.800	1.000	1.000	0.083
Gemmatimonas	0.023	0.167	0.143	0.000	0.000	0.000	0.000	0.000	0.083
Enhydrobacter	0.045	0.000	0.286	0.000	0.000	0.400	0.125	0.167	0.083
Caulobacter	0.000	0.000	0.143	0.167	0.000	0.000	0.000	0.167	0.077
Neisseria	0.000	0.167	0.143	0.000	0.000	0.000	0.000	0.000	0.077
Marmoricola	0.023	0.000	0.286	0.000	0.000	0.000	0.000	0.000	0.077
Saccharopolyspora	0.000	0.000	0.286	0.000	0.000	0.000	0.000	0.000	0.071
Serratia	0.000	0.000	0.286	0.000	0.000	0.000	0.000	0.000	0.071
Limnohabitans	0.091	0.000	0.000	0.167	0.000	0.000	0.000	0.000	0.064
Micrococcus	0.114	0.000	0.143	0.000	0.000	0.200	0.000	0.000	0.064
Chryseobacterium	0.091	0.000	0.143	0.000	0.167	0.000	0.000	0.000	0.058
Alistipes	0.045	0.167	0.000	0.000	0.000	0.000	0.000	0.000	0.053
Thermobacillus	0.045	0.000	0.000	0.167	0.000	0.000	0.000	0.000	0.053
Bacillus	0.068	0.000	0.143	0.000	0.167	0.200	0.000	0.000	0.053
Rubrobacter	0.068	0.000	0.143	0.000	0.000	0.000	0.000	0.000	0.053
Brucella	0.023	0.000	0.000	0.167	0.000	0.000	0.000	0.000	0.047
Diaphorobacter	0.023	0.000	0.000	0.167	0.167	0.200	0.000	0.000	0.047
Lachnoclostridium	0.023	0.000	0.000	0.167	0.000	0.000	0.000	0.000	0.047
Pediococcus	0.023	0.167	0.000	0.000	0.000	0.000	0.000	0.000	0.047
Pyrinomonas	0.023	0.167	0.000	0.000	0.000	0.200	0.000	0.000	0.047
Solirubrobacter	0.023	0.167	0.000	0.000	0.000	0.000	0.000	0.000	0.047
UCG 002	0.023	0.000	0.000	0.167	0.000	0.000	0.125	0.000	0.047
Candidatus Udaeobacter	0.045	0.000	0.143	0.000	0.000	0.000	0.000	0.000	0.047
Dechloromonas	0.045	0.000	0.143	0.000	0.333	0.000	0.000	0.167	0.047
Gordonia	0.045	0.000	0.143	0.000	0.000	0.000	0.000	0.000	0.047
nthomonas	0.045	0.000	0.143	0.000	0.167	0.000	0.000	0.000	0.047
Acetatifactor	0.000	0.167	0.000	0.000	0.000	0.000	0.000	0.000	0.042
Amycolatopsis	0.000	0.167	0.000	0.000	0.000	0.000	0.000	0.000	0.042
Bergeyella	0.000	0.000	0.000	0.167	0.000	0.000	0.000	0.000	0.042
Candidatus Methylopumilus	0.000	0.167	0.000	0.000	0.000	0.000	0.125	0.000	0.042
Devosia	0.000	0.000	0.000	0.167	0.167	0.000	0.000	0.000	0.042
Eubacterium xylanophilum group	0.000	0.000	0.000	0.167	0.167	0.000	0.000	0.000	0.042
Haloquadratum	0.000	0.000	0.000	0.167	0.000	0.000	0.000	0.000	0.042
Lachnospiraceae AC2044 group	0.000	0.000	0.000	0.167	0.000	0.000	0.000	0.000	0.042

Lachnospiraceae NK4A136 group	0.000	0.167	0.000	0.000	0.000	0.000	0.125	0.000	0.042
Listeria	0.000	0.000	0.000	0.167	0.000	0.000	0.000	0.000	0.042
Neochlamydia	0.000	0.167	0.000	0.000	0.000	0.000	0.000	0.000	0.042
Pedomicrobium	0.000	0.167	0.000	0.000	0.000	0.000	0.000	0.000	0.042
Peribacillus	0.000	0.000	0.000	0.167	0.000	0.000	0.000	0.000	0.042
Planococcus	0.000	0.167	0.000	0.000	0.000	0.200	0.000	0.000	0.042
Pseudolabrys	0.000	0.000	0.000	0.167	0.167	0.000	0.000	0.000	0.042
Puia	0.000	0.000	0.000	0.167	0.000	0.000	0.000	0.000	0.042
Rhodoferax	0.000	0.167	0.000	0.000	0.000	0.000	0.000	0.000	0.042
Roseburia	0.000	0.167	0.000	0.000	0.000	0.000	0.000	0.000	0.042
Roseiarcus	0.000	0.167	0.000	0.000	0.000	0.000	0.000	0.000	0.042
Shuttleworthia	0.000	0.167	0.000	0.000	0.000	0.000	0.000	0.000	0.042
Sphingobacterium	0.000	0.167	0.000	0.000	0.000	0.000	0.000	0.167	0.042
Sphingobium	0.000	0.167	0.000	0.000	0.000	0.000	0.000	0.000	0.042
UCG 005	0.000	0.167	0.000	0.000	0.000	0.000	0.000	0.000	0.042
Baekduia	0.023	0.000	0.143	0.000	0.000	0.000	0.000	0.000	0.041
Blastococcus	0.023	0.000	0.143	0.000	0.333	0.000	0.000	0.000	0.041
Cloacibacterium	0.023	0.000	0.143	0.000	0.000	0.000	0.000	0.000	0.041
Hymenobacter	0.023	0.000	0.143	0.000	0.000	0.000	0.000	0.000	0.041
Jatrophihabitans	0.023	0.000	0.143	0.000	0.000	0.000	0.000	0.000	0.041
Lichenibacterium	0.023	0.000	0.143	0.000	0.000	0.000	0.000	0.000	0.041
Niallia	0.023	0.000	0.143	0.000	0.000	0.000	0.000	0.000	0.041
Paenibacillus	0.023	0.000	0.143	0.000	0.000	0.000	0.000	0.333	0.041
Pseudonocardia	0.023	0.000	0.143	0.000	0.000	0.000	0.000	0.000	0.041
Reyranella	0.023	0.000	0.143	0.000	0.000	0.000	0.000	0.000	0.041
Treponema	0.023	0.000	0.143	0.000	0.000	0.000	0.000	0.000	0.041
Cutibacterium	0.159	0.000	0.000	0.000	0.000	0.400	0.000	0.000	0.040
Aggregatibacter	0.000	0.000	0.143	0.000	0.000	0.000	0.000	0.000	0.036
Alteribacter	0.000	0.000	0.143	0.000	0.000	0.000	0.000	0.000	0.036
Caldovatus	0.000	0.000	0.143	0.000	0.000	0.000	0.000	0.000	0.036
Candidatus Alysiosphaera	0.000	0.000	0.143	0.000	0.000	0.000	0.125	0.000	0.036

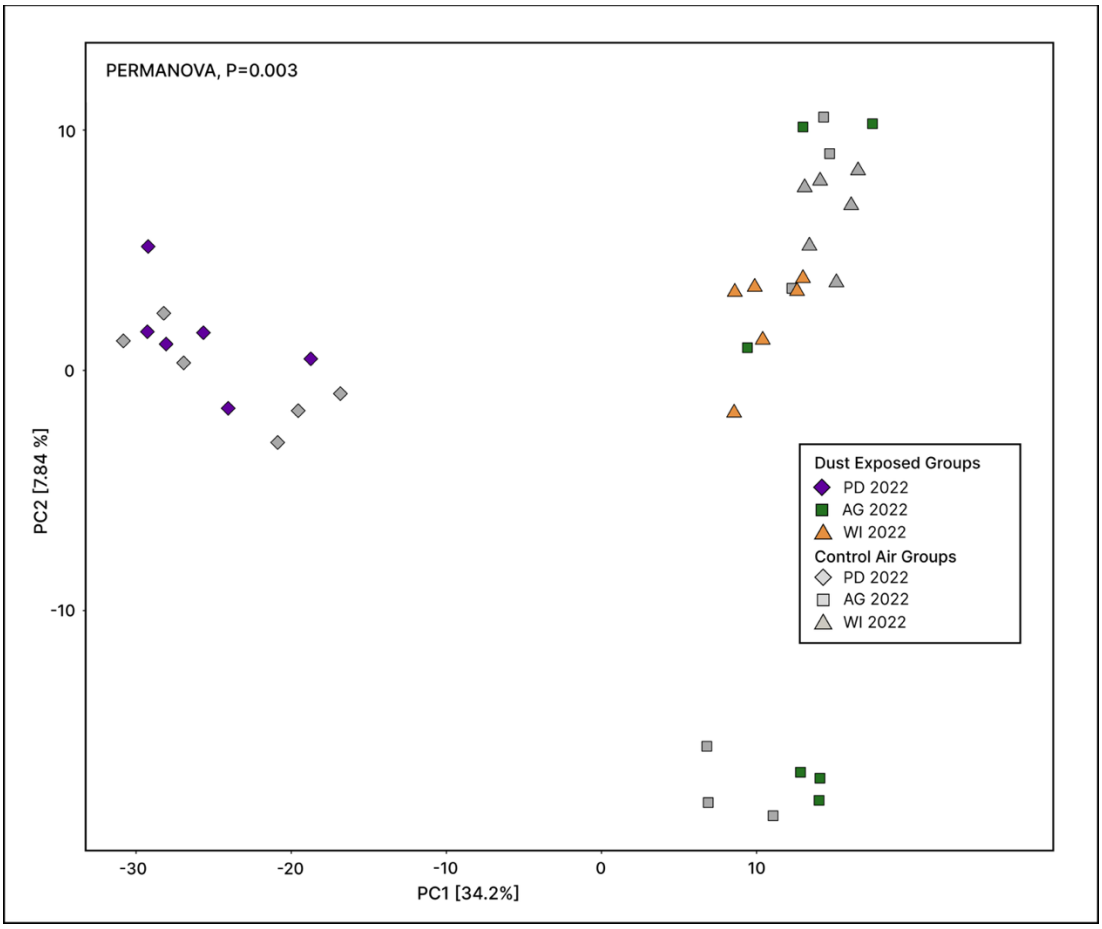

Fig S2.2 PCoA of fecal microbiome composition by treatment group using CLR-transformed (Aitchison) distances

CHAPTER III

Title: Visualizing the Dispersion and Clearance of Staphylococcus aureus in the Murine Lung

Abstract

The previous belief in lung sterility had been motivated by the robust clearance mechanisms in place to prevent foreign pathogens from the environment into the respiratory tract. However, is it now considered that these same clearance mechanisms work to maintain the steady-state lung microbiome. In this chapter, we hypothesized that if clearance is favored following the introduction of live bacterial cells through the nasal passage, we would observe reduced bacterial signal over 48-hrs post-exposure. We compare methods of viable bacterial introduction into the murine respiratory tract to observe bacterial dispersion and clearance in the lung. We utilized intranasal exposure, direct lung inflation, and aerosolization to expose C57BL/6 mice to *Staphylococcus aureus* UAMS-1 pCM29, a clinically isolated strain with a transformed plasmid for constitutive cytosolic green fluorescent protein (GFP) expression. It was determined that intranasal exposure was the most effective at introducing *S. aureus* into the lung at concentrations that were high enough for subsequent visualization in fluorescent microscopy. It was also found that bacterial cells were cleared from the lung by 48-hrs post-exposure. This chapter outlines basic methods for *in situ* bacterial visualization in lung tissues and demonstrates how these methods can be used to qualitatively observe clearance of a bacterial strain over time. Based on our findings, we speculate that eventual infection or disruption to the lung microbiome must occur under competitive pressures that subsequently overwhelm host pulmonary clearance mechanisms.

Introduction

In my previous two chapters, environmental dust material was filtered through a 0.2um mesh before aerosolization in the environmental chamber. The final aerosols are abiotic, with no direct exposure to viable bacterial cells occurring over the course of the experiment. Yet, this approach demonstrates the efficacy of abiotic dust exposures for observing consequential inflammation and microbiome shifts. This does not directly mimic natural systems, as viable microorganisms are ubiquitous in the environment and thus susceptible to mammalian inhalation (1). Likewise, it is assumed that mammalian hosts are equipped with robust clearance mechanisms that ensure foreign pathogens are dispelled from the respiratory tract before they have the chance to proliferate. These mechanisms are what had previously motivated the belief that the lung was a sterile environment; however, we know now that the lung microbiome is primarily maintained in a steady-state, with very little opportunity for immigration and subsequent colonization in the lower respiratory tract (LRT) despite directly interfacing with environmental aerosols (2–4).

Microaspiration, aerosol inhalation, and dispersion across mucosal surfaces motivates microbial immigration into the lungs. Upon arrival, however, microbes must survive the stringent ecology of the lung defined by variable oxygen availability, pH, wide spatial variation, and low nutrient availability (5). Meanwhile, innate immune cell populations and mucociliary mechanisms– which directly target microbial cells for clearance– further threaten microbial survival (6). A clinical study by Dickson et. al suggests that lung bacterial topography of healthy patients conform to an “adapted island

model", where immigration (by microaspiration) and elimination are primarily responsible for maintaining community balance as opposed to selective pressures by the lung (7).

For bacteria in the *Staphylococcus* genus, studies have found that increased *Staphylococcus* loads tend to be associated with disease-state lung microbiomes; however, others note that inoculation of *S. aureus* into the lung was protective against infectious pneumonia challenge (8). Overall, the potential of *Staphylococcus spp.* to exist in the lungs of both healthy and diseased patients led us to assume that exposure to *S. aureus* would effectively demonstrate post-exposure dispersion and subsequent clearance or proliferation in the lung. We hypothesize that if clearance is favored following introduction of live bacterial cells through the nasal passage, we would observe reduced bacterial signal (via microscopy and viable cell counts) with increased time post-exposure.

Minimal methods have been described for administering and visualizing viable microbial cells in the host respiratory tract. In infection models, *Streptococcus pneumoniae* transformed with a *lux* plasmid for bioluminescence has been used to visualize *in vivo* progression of pneumococcal infection and subsequent reduction after antibiotic treatment with photon emission imaging on live mice (9). Additional studies have utilized intranasal or nebulizer-based aerosolization paired with tissue homogenization for viable colony-forming unit (CFU) counts to determine post-exposure bacterial viability (10,11). While these methods have demonstrated potential for understanding the course of bacterial infection in the respiratory tract, the methods

described in this chapter set out to visualize bacterial cell dispersion in the lung tissue following various modes of introduction.

Methods

Bacterial Strain Use and Maintenance

Staphylococcus aureus UAMS-1 pCM29 is a clinically isolated strain with a transformed plasmid for constitutive cytosolic green fluorescent protein (GFP) expression (12,13). We maintained *S. aureus* UAMS-1 pCM29 cultures in LB (Lysogeny Broth) media containing chloramphenicol for plasmid maintenance. Long-term cultures were suspended in 1:1 volume with 50% glycerol and stored at -80C.

Animal Use Ethics

All work involving the use of live mice was done in compliance with the University of California, Riverside's Institutional Animal Care and Use Committee (IACUC) and National Institute of Health (NIH) guidelines. Male C57BL/6 mice were purchased from Jackson Labs (Sacramento, CA) at 8 weeks old. Mice were acclimated for approximately one week in a specific-pathogen free vivarium (University of California, Riverside) before use in our chamber exposure studies.

Microbial Exposures

Lung inflation was performed on 10-13 week old C57BL/6 mice after isoflurane euthanasia and cervical dislocation. The chest cavity and throat were exposed to visualize

the lungs to the trachea. A small piercing was made on the ventral side of the trachea with a sterile 21G needle before sterile tubing was inserted through the trachea. A syringe containing 0.8mL of liquid *S. aureus* culture (OD_{600}=0.06-0.1) was attached to the tubing and used to inflate the lung. The trachea was tied off then the lung was extracted, and lobes were separated for histology.

Mice exposed intranasally were sedated with isoflurane before receiving 50uL of *S. aureus* UAMS-1 pCM29 liquid culture in LB (approx. 10^7 CFU/mL) via right or left nostril. Mice were left to "rest" for 1 hr (T_1), 24 hr (T_2), or 48 hrs (T_3). Resting mice were assigned to lidded cages and provided with food and water as needed. Cages of mice resting overnight (T_2 and T_3 groups) were left in larger chamber enclosures cycling dry, filtered air with a 12 hr light/dark cycle, and maintaining an average temperature of 25ºC and <70% relative humidity. Unexposed, control mice (T_0) were used as a comparison for downstream imaging.

Aerosol exposures were performed in a 12x12x12" chamber system modified from Peng et. al (14), as discussed in previous chapters. Bacterial solution in 0.9% saline was prepared with approximately 10^9 CFU/mL of *S. aureus* liquid culture (OD_{600}=0.06-0.1). The solution was left on a stir/heat plate (37ºC) to facilitate bacterial viability. The liquid solution was passed through an atomizer which included a silica drying column and heating coil to reduce relative humidity in the chamber. The final aerosol solution was mixed with dilution air at 1 liter per minute over the course of the exposure period to maintain an even flow of air into the chamber. The exhaust line was split between a HEPA filter and an input into LAP 322 Aerosol Spectrometer (Topas GmbH, Dresden,

Germany) to monitor live particle size distribution over the course of the exposure period. These exposures were carried out with a maximum of four C57BL/6 mice for up to 48 hours in a 12hr/12hr dark/light cycle with food and water provided.

Lung Tissue Dissection

Mice were euthanized with isoflurane and cervical dislocation as per humane animal use protocols. For a subset of samples, the whole lung was extracted, then homogenized in 5mL of 1x phosphate-buffered saline (PBS). Undiluted homogenate was spread plated (50uL) on selective LB-chloramphenicol media then incubated at 37ºC to determine viable colony counts for the whole lung of each mouse.

For histology mice, the left and right lobes were separated at the tracheal bifurcation and suspended in 4% paraformaldehyde (PFA). After overnight fixation, samples were washed twice for 10 minutes in 1x PBS, then transferred to 30% sucrose overnight. Fixed tissue samples were mounted in optimal cutting temperature (OCT) compound and stored at -20C before slicing.

Histology Sectioning, Staining, and Imaging

Tissue sections were sliced at 12um on the RWD FS800 Cryostat (RWD Life Science Co., Shenzhen, China). Left lung lobes were sectioned starting at the ventral side to prioritize major airway visualization. Slides were mounted with ProLong Gold Antifade Mountant with DNA Stain DAPI (Invitrogen, Carlsbad, CA) and visualized under fluorescent microscopy using the Keyence BZ-X800 (Keyence Corporation, Itasca,

IL). DAPI blue fluorescence was used to differentiate mammalian tissue autofluorescence from *S. aureus* fluorescence in the green fluorescence channel.

Results

Visualizing S. aureus In Situ

Shape, size, and magnitude of *S.aureus* UAMS-1 pCM29 was first verified using a wet mount visualized with green fluorescent microscopy (Fig. 3.1A). Inflated and intranasally exposed mouse lungs were compared against an unexposed control mouse (Fig. 3.1B) to differentiate bacterial GFP signal from tissue autofluorescence (Fig. 3.1C), then overlaid with DAPI images to contrast bacterial signal from mammalian cells. We visualized ample bacterial GFP signals from both inflated lungs (Fig. 3.2A) and intranasally exposed mice (Fig. 3.2C). However, in the inflated lung, bacterial signals appeared to be more clustered around airways and along the perimeter of the lobe. In contrast, intranasally exposed lungs displayed a wider dispersal of cells in the upper portion of the lobe. Despite differences in dispersion patterns, we were able to visualize introduction of viable bacterial cells into the lung and subsequent maintenance of cell viability through the histological sectioning and staining processes.

Clearance of S. aureus 48-hours After Intranasal Exposure

Lung tissues were collected at 1- (T_1), 24- (T_2), and 48-hrs (T_3) after intranasal exposure. Left lobes were visualized in both green fluorescence and DAPI channels to contrast host and microbial fluorescent signals. At 1-hr after intranasal exposure, we were

able to clearly visualize *S. aureus* cell distribution and clustering in lung tissues, with no biases around major airways or other geographic features of the left lobe (Fig. 3.3A). At 24-hrs after intranasal exposure, most bright GFP signals were overlapping with similar signals in the DAPI channel, indicating that these clusters were likely not unique to *S. aureus* presence in the lung (Fig. 3.3B). While some areas did display scattered GFP signals at a comparable size and shape to those found in T_1 mice, these signals were less ubiquitous in comparison. By 48-hrs after intranasal exposure, no *S. aureus* cells could be visualized in the lung tissue, suggesting that bacterial cells were successfully cleared and no longer viable in these mice (Fig. 3.3C).

Colony counts from tissue homogenate were taken to postulate *S. aureus* viability from each exposure group. On average, T_1 whole-lung homogenate was found to have approximately 13 CFU/mL. Similarly, T_2 whole-lung homogenate had, on average, 13 CFU/mL. T_3 homogenate returned no viable colonies from whole lung homogenate.

Comparing Methods of Viable Bacterial Exposure

Intranasal exposure with *S. aureus* liquid culture successfully introduced viable bacterial cells into the mouse lung. Similarly, post-euthanasia inflation of mouse lungs was also sufficient in introducing bacterial cells directly into the lower respiratory tract; however, the dispersion of bacteria between these methods varied (Fig. 3.2). Presence of *S. aureus* in the lung was able to be visualized under green fluorescent microscopy indicating that bacterial cells stayed viable through the exposure and histology process.

In contrast, lungs retrieved from aerosol-exposed mice did not display any distinct bacterial signals after 24- or 48-hrs of exposure (Fig. 3.4). We were able to verify that bacterial cells maintained viability through the aerosolization process after growth on exposed solid media dishes. Despite no fold change in CFU/mL between the starting bacterial saline solution ($500x10^9$ CFU/mL) and the calculated average CFU on media plates after 24hrs of exposure ($300x10^9$ CFU/mL), this rate of bacterial dispersion in the chamber did not translate to successful introduction in the murine respiratory tract when visualized.

Discussion

In this chapter, we first set out to compare three methods of bacterial aerosol administration using fluorescent *S. aureus* UAMS-1 pCM29: intranasal, inflation, and aerosolization. After each mode of introduction, lungs were visualized using fluorescent microscopy. Intranasal exposure of bacterial culture in broth (50uL, ~10^7-10^9 CFU/mL) was consistently successful, with bacterial cells clearly visible in the lung at 1-hr after exposure (Fig. 3.1). In contrast, other modes of viable cell introduction were deemed to be less sufficient in tracking bacterial dispersion. While post-euthanasia inflation was successful in introducing bacterial cells into the lung tissue (Fig. 3.2A), this method is limited and cannot effectively track bacterial patterns *in vitro* through time. While controlled aerosolization of *S. aureus* culture was successful in maintaining bacterial viability, this did not translate to visibility in the lungs of exposed mice.

Previous research on microsphere deposition in the lung compared the efficacy of intranasal vs. aerosol exposures for even dispersion throughout the lung (15). It was found that intranasally-administered microspheres tended to cluster unevenly in and around major airways of the lung while aerosol-administered microspheres were more evenly dispersed throughout the lung tissue. Regardless of dispersion efficacy, successful introduction of microspheres was observed by both routes of administration. Because our methods of aerosolization were confirmed to maintain bacterial viability, these findings lead us to speculate that respiratory rates and host clearance mechanisms in the lung prevent concentrated bioaerosols from infiltrating the lower respiratory tract. A study comparing the aerosolization of four bacterial species (*Enterobacter cloacae, Erwinia herbicola, K. planticola, and P. syringae*) described that relative humidity and aerosol temperature played a significant role in bacterial survivability in the airspace (16). However, the conditions described in this paper tracked exposure through the airspace alone, and therefore did not account for mammalian respiratory introduction. Similar aerosol-based methods for introducing bacteria into the host respiratory tract would likely require a much more concentrated solution in conjunction with appropriate airspace conditions to accommodate for both bacterial and mammalian survival.

We then utilized intranasal exposures to administer and visualize bacterial clearance in the lung after 1-, 24-, and 48- hrs. It was hypothesized that if the lung preferentially favors bacterial clearance after a concentrated bacterial load is introduced, then reduced bacterial signal and viable counts would be observed over time. It was found that bacterial signal in the lung is widely reduced by 24hrs, demonstrating that

clearance is likely occurring at a faster rate than *S. aureus* proliferation (Fig. 3.3). Among intranasally exposed mice, however, an equal average of 13CFU/mL counts were observed after 1- and 24-hrs post-exposure, while zero CFUs were observed for 48-hrs post-exposure mice. While these counts were relatively low for total lung homogenate (17), presence of viable bacteria in both treatment groups suggest that viable *S. aureus* was present in the lung of intranasally exposed mice after 24-hrs, despite the visibility of these cells being less definitive in comparison to lobes taken 1-hr after exposure. One possible explanation for this discrepancy is an unequal distribution of *S. aureus* in the lung by intranasal exposure, as previously noted (15), which over the course of 24-hrs, may have enabled particular "pockets" of bacterial cells to remain or be expelled to extracellular spaces. In a study comparing clearance of *S. aureus* in bronchoalveolar lavage fluid vs. lung samples over the course of 24-hrs, researchers found that clearance of bacterial cells in lung tissue occurs much more rapidly than in bronchial spaces, with a majority of recovered *S. aureus* 6-hrs post-exposure coming from lavage collections. However, these findings were noted to disagree with previous work in which *S. aureus* clearance in the lung was shown to occur at uniform rates, regardless of intra- or extracellular location (17–19). It is possible that *S. aureus* that had migrated or remained in the airways 24-hours after exposure would be inaccurately excluded from visualization.

This chapter applies various exposure methods for direct introduction of *Staphylococcus aureus* into the mouse respiratory tract and subsequent observation of bacterial clearance; however, variability between infectious doses of other bacterial

strains would require these methods to be adapted accordingly. A study examining the protective potential of a recurring intranasal exposure of *Lactobacillus spp.* against influenza virus noted that acute exposures to live or dead *Lactobacillus rhamnosus* at 10^8 CFU/mL lead to pneumonia symptoms (20). Another study found that the 50% lethal dose of intranasally administered *Pseudomonas aeruginosa* was at the magnitude of 10^7 CFU/mL, while a 10^8 CFU/mL dose of *Pseudomonas cepacia* was cleared by the 7th day post-exposure (11).

As we aim to elucidate the patterns and function of the lung microbiome and how it interacts with exposure-based input, it is likely that specific regulative functions of the existing lung microbiome will be revealed. By qualitatively examining the effects of directly introducing viable bacteria into the lung, we infer that the observed clearance of *S. aureus* within 48 hours reflects the lung's tendency to preserve the existing microbial community by removing foreign microbes. This is in line with the "adaptive island model" proposed by Dickson et al. (7), which suggessts that regular migration and clearance of microbes maintains the dynamics of the existing lung microbial community. Therefore, we can speculate that eventual infection or disruption to the lung microbiome must occur under competitive pressures that subsequently overwhelm host pulmonary clearance mechanisms.

List of Figures

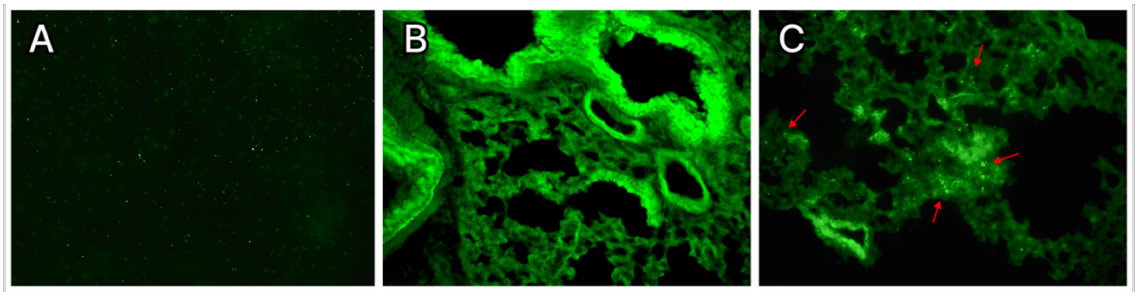

Figure 3.1 Bacterial GFP signal in comparison to tissue autofluorescence. (A) *Staphylococcus aureus* UAMS-1 pCM29 visualized at 20x magnification under green fluorescence in comparison to **(B)** green autofluorescence of control lung (T_0) imaged at 20x magnification. **(C)** *S. aureus* visualized 1-hr after intranasally exposed lung tissue at 20x magnification under green fluorescent microscopy demonstrates detectable signal of *S. aureus* over tissue autofluorescence.

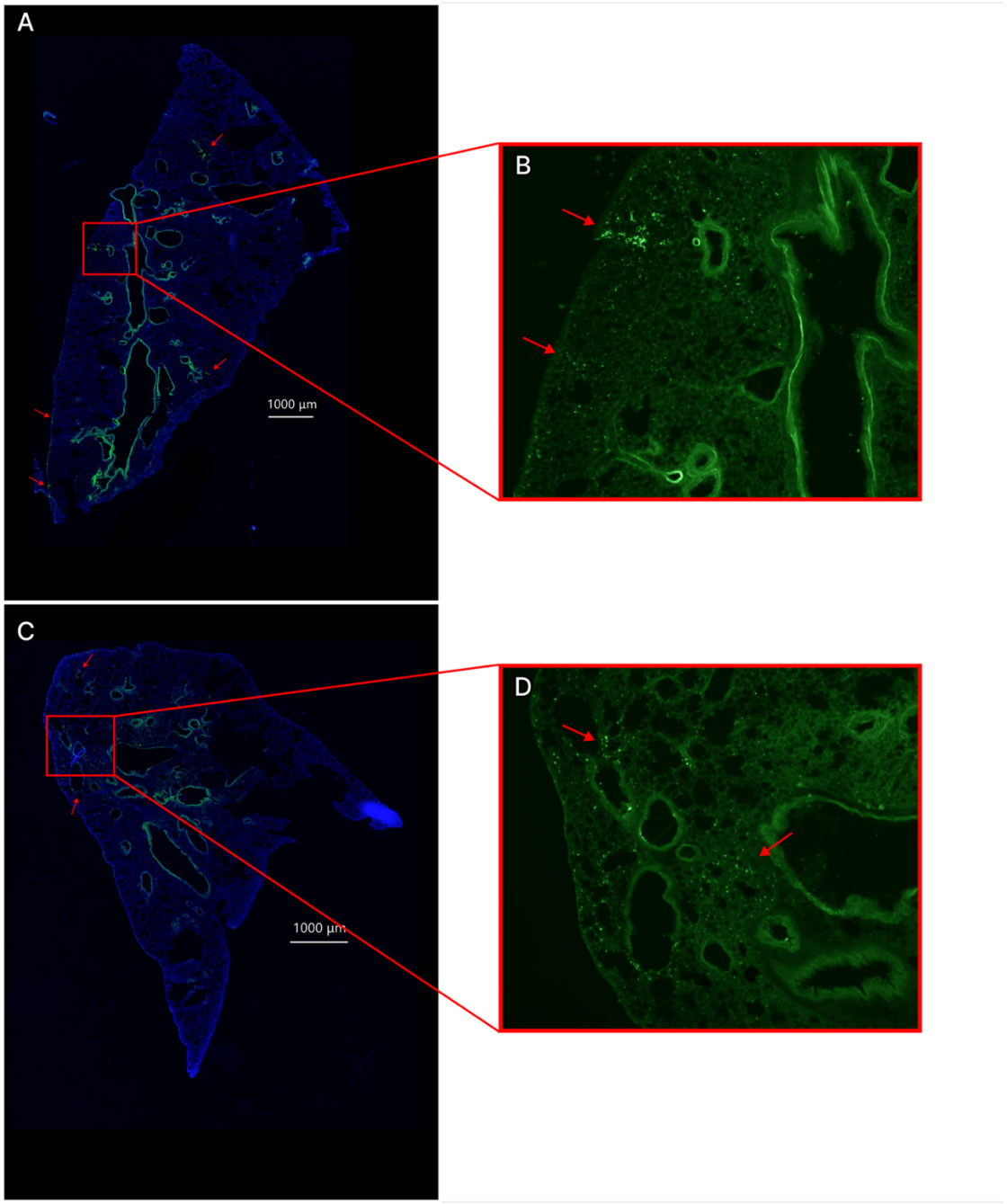

Figure 3.2 Comparison of *S. aureus* dispersion in the full left lobes of mice after **(A)** inflation and **(C)** intranasal exposure. DAPI and green fluorescence channel images were overlayed to contrast host and microbial fluorescent signals. Zoomed in panels **(C,D)** highlight *S. aureus* presence visualized in the green fluorescence channel at 4x magnification. Red arrows highlight prominent clusters of *S. aureus*.

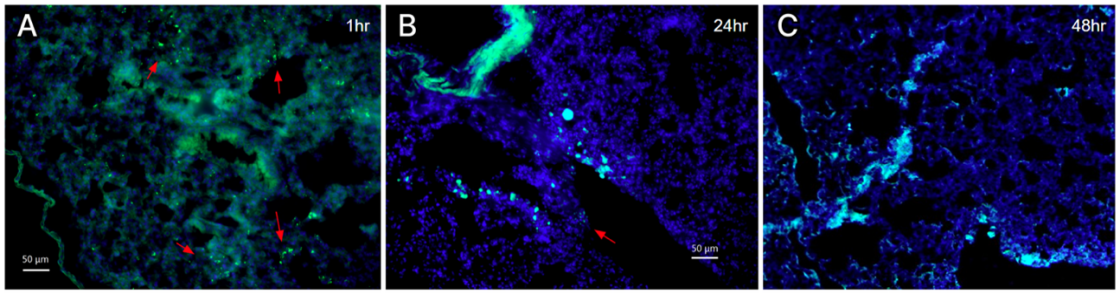

Figure 3.3 Lung tissues visualized at 20x magnification after intranasal exposure at **(A)** 1-hr (T_1), **(B)** 24-hrs (T_2), and **(C)** 48-hrs (T_3) after intranasal exposure to *S. aureus*. Green fluorescence and DAPI channels were overlayed to contrast host and microbial signals, and arrows highlight prominent clusters of *S. aureus* signal. Average CFU/mL counts post-exposure were T_1=13 CFU/mL, T_2=13 CFU/mL, T_3=0 CFU/mL.

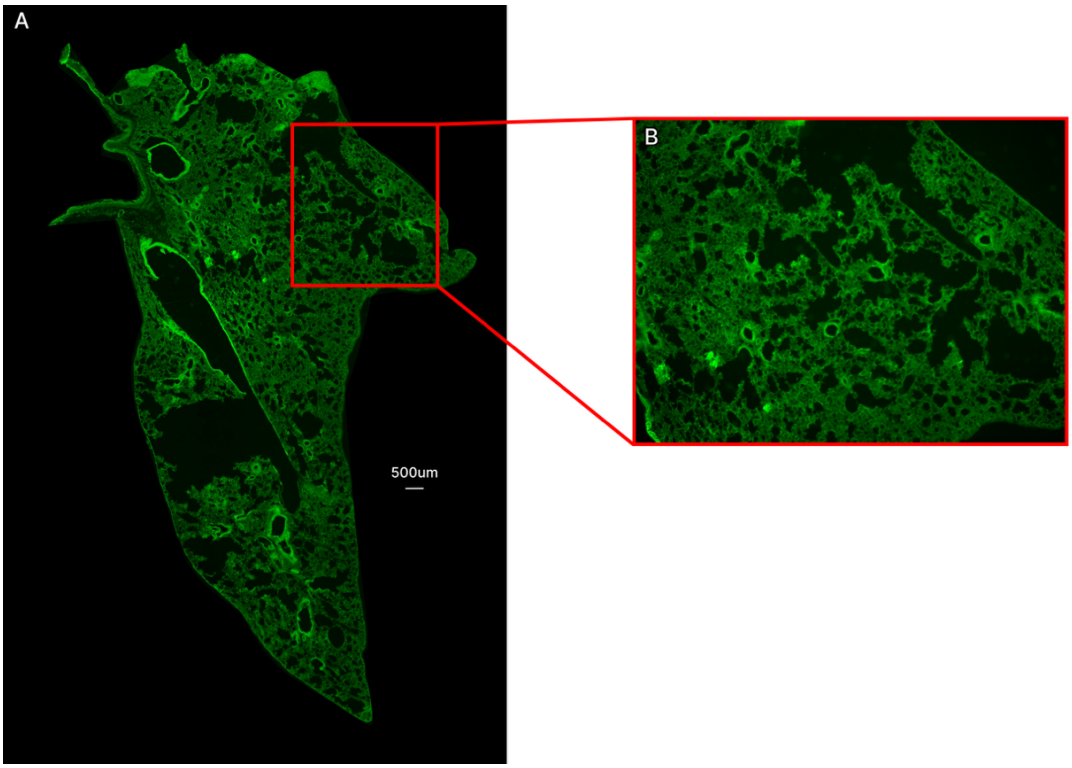

Figure 3.4 Lung tissue visualized after aerosol exposure to *S. aureus*. (A) Full left lobe taken post-aerosol exposure to *S. aureus* visualized in the green fluorescence channel. **(B)** Highlighted section at 4x magnification displays no visible clustering of *S. aureus*.

References

1. McCumber AW, Kim YJ, Isikhuemhen OS, Tighe RM, Gunsch CK. The environment shapes swine lung bacterial communities. Sci Total Environ. 2021 Mar;758:143623.

2. Hilty M, Burke C, Pedro H, Cardenas P, Bush A, Bossley C, et al. Disordered Microbial Communities in Asthmatic Airways. Neyrolles O, editor. PLoS ONE. 2010 Jan 5;5(1):e8578.

3. Charlson ES, Bittinger K, Haas AR, Fitzgerald AS, Frank I, Yadav A, et al. Topographical Continuity of Bacterial Populations in the Healthy Human Respiratory Tract. Am J Respir Crit Care Med. 2011 Oct 15;184(8):957–63.

4. Marimón JM. The Lung Microbiome in Health and Respiratory Diseases. Clin Pulm Med. 2018 Jul;25(4):131–7.

5. Dickson RP, Erb-Downward JR, Martinez FJ, Huffnagle GB. The Microbiome and the Respiratory Tract. Annu Rev Physiol. 2016 Feb 10;78(1):481–504.

6. Whiteside SA, McGinniss JE, Collman RG. The lung microbiome: progress and promise. J Clin Invest. 2021 Aug 2;131(15):e150473.

7. Dickson RP, Erb-Downward JR, Freeman CM, McCloskey L, Falkowski NR, Huffnagle GB, et al. Bacterial Topography of the Healthy Human Lower Respiratory Tract. Clemente JC, editor. mBio. 2017 Mar 8;8(1):e02287-16.

8. Wypych TP, Wickramasinghe LC, Marsland BJ. The influence of the microbiome on respiratory health. Nat Immunol. 2019 Oct;20(10):1279–90.

9. Francis KP, Yu J, Bellinger-Kawahara C, Joh D, Hawkinson MJ, Xiao G, et al. Visualizing Pneumococcal Infections in the Lungs of Live Mice Using Bioluminescent *Streptococcus pneumoniae* Transformed with a Novel Gram-Positive *lux* Transposon. Tuomanen EI, editor. Infect Immun. 2001 May;69(5):3350–8.

10. Laurenzi GA, Berman L, First M, Kass EH. A Quantitative Study of the Deposition and Clearance of Bacteria in the Murine Lung*. J Clin Invest. 1964 Apr 1;43(4):759–68.

11. George SE, Kohan MJ, Whitehouse DA, Creason JP, Kawanishi CY, Sherwood RL, et al. Distribution, clearance, and mortality of environmental pseudomonads in mice upon intranasal exposure. Appl Environ Microbiol. 1991 Aug;57(8):2420–5.

12. Sassi M, Sharma D, Brinsmade SR, Felden B, Augagneur Y. Genome Sequence of the Clinical Isolate Staphylococcus aureus subsp. aureus Strain UAMS-1. Genome Announc. 2015 Feb 26;3(1):e01584-14.

13. De Jong NWM, Van Der Horst T, Van Strijp JAG, Nijland R. Fluorescent reporters for markerless genomic integration in Staphylococcus aureus. Sci Rep. 2017 Mar 7;7(1):43889.

14. Peng X, Maltz MR, Botthoff JK, Aronson EL, Nordgren TM, Lo DD, et al. Establishment and characterization of a multi-purpose large animal exposure chamber for investigating health effects. Rev Sci Instrum. 2019 Mar 1;90(3):035115.

15. Yisrael K, Drover RW, Shapiro ML, Anguiano M, Kachour N, Li Q, et al. Route of administration significantly affects particle deposition and cellular recruitment. Omri A, editor. PLOS ONE. 2023 Nov 27;18(11):e0289373.

16. Marthi B, Fieland VP, Walter M, Seidler RJ. Survival of bacteria during aerosolization. Appl Environ Microbiol. 1990 Nov;56(11):3463–7.

17. Goldstein E, Lippert W, Warshauer D. Pulmonary Alveolar Macrophage DEFENDER AGAINST BACTERIAL INFECTION OF THE LUNG. J Clin Invest. 1974 Sep 1;54(3):519–28.

18. Nugent KM, Pesanti EL. Nonphagocytic clearance of Staphylococcus aureus from murine lungs. Infect Immun. 1982 Jun;36(3):1185–91.

19. Green GM, Kass EH. THE ROLE OF THE ALVEOLAR MACROPHAGE IN THE CLEARANCE OF BACTERIA FROM THE LUNG. J Exp Med. 1964 Jan 1;119(1):167–76.

20. Youn HN, Lee DH, Lee YN, Park JK, Yuk SS, Yang SY, et al. Intranasal administration of live Lactobacillus species facilitates protection against influenza virus infection in mice. Antiviral Res. 2012 Jan;93(1):138–43.

Conclusion

Within the last decade, culture-independent techniques have revealed the presence of a distinct microbial community in the lower respiratory tract of healthy individuals. It's been found that the healthy lung microbiome develops in tangent to the immune system and serves an important role in immune regulation and pathway signaling (1–3). Though plenty of clinical studies have sought to determine how lung microbiome composition and diversity correlate with common pulmonary diseases like asthma, cystic fibrosis, and COPD, our work aims to reveal changes in the lung microbiome that are associated with inflammatory environmental dust exposures.

In the first chapter, we exposed mice to environmental dust collected from the Salton Sea basin in California's Imperial Valley, which had been previously shown to induce acute neutrophilic inflammatory responses (4,5). It was revealed that lung microbiome diversity and composition changed in response to environmental dust exposure; however, decreases in diversity and evenness were not directly correlated with the magnitude of neutrophil recruitment in the lung.

In the second chapter, we demonstrated how spatiotemporal variation in environmental dust material collected from three different Salton Sea sites in 2020-2022 significantly changes lung microbiome composition and evenness. Among dust-exposed mice, we determined that a significant decrease in fecal microbiome diversity was correlated to significantly increased diversity in the lung microbiome. This highlights potential mediation by way of the gut-lung axis in response to pulmonary inflammation induced by chronic exposure to environmental dust.

The third chapter compared methods for introducing viable *Staphylococcus aureus* into the mouse lung. We found that intranasal exposures were most effective for downstream *in situ* visualization of viable bacteria in the lung tissue. This method was then used to visualize the eventual clearance of GFP-tagged *S. aureus* over 48-hrs post-intranasal exposure. These findings suggest that exposure to a known lung-associated microbe does not directly result in lung colonization. Instead, preferential clearance of *S. aureus* aligns with Dickson et. al's "adapted island" model of lung biogeography, in which regular migration and clearance of bacteria from the respiratory tract are more influential in maintaining the healthy lung microbiome in comparison to bacterial survivability and subsequent proliferation against the lung's selective pressures (6).

Altogether, our findings show that the lung microbiome is responsive to variable characteristics of environmental dust after chronic exposure. We observed that inflammation induced by exposure is more consistently associated with the dust collection site, while changes in the lung microbiome vary more by season of collection. Among dust exposures that lead to higher neutrophil recruitment, changes in lung microbiome composition are evident. However, significant shifts in the lung microbiome are not consistently correlated with increased neutrophil recruitment. This suggests that the lung microbiome may respond directly to the composition of the dust itself, rather than solely to inflammation-related biochemical changes in the lung. In a study by Lin et. al, researchers found that lung microbiome composition was significantly variable according to patient location (7). While they observed no link between microbiome composition and susceptibility to COPD-related risk factors like smoking or $PM_{2.5}$

exposure, our results suggest that repeated exposure to environmental dusts from specific sites and seasons can shape lung microbiome composition and diversity. Exactly how these changes in the microbiome facilitate pulmonary inflammation is not yet understood. Therefore, it would be valuable to further investigate if certain characteristics of the lung microbiome make one more reactive to environmental dust exposures.

In the case of the Salton Sea basin, poor environmental management, increased industrial activity, and climate change are contributing to more extreme dust events (8–11) in a region that experiences disproportionately high rates of childhood asthma when compared to the average state and national rates (12,13). Here, we demonstrate a relationship between environmental dust exposure, host pulmonary health, and the host microbiome in which chronic exposure to environmental dust from a particular site and season can have differential effects on pulmonary inflammation and the host microbiomes. Subsequent investigation of the total lung microbiome (bacteriome, mycobiome, and virome) may give further insight into the functional characteristics relevant to pulmonary inflammation and chronic environmental exposures. Additionally, examining metabolic activity along the gut-lung axis may reveal the potential of utilizing the host microbiome in interventions for environmentally induced pulmonary inflammation. As air pollution increases in both rural and urban communities, it will be necessary to understand the nuanced ways of how we interact with and respond to our lived environment to develop effective public health strategies and improve respiratory health outcomes.

References

1. Hilty M, Burke C, Pedro H, Cardenas P, Bush A, Bossley C, et al. Disordered Microbial Communities in Asthmatic Airways. Neyrolles O, editor. PLoS ONE. 2010 Jan 5;5(1):e8578.

2. Kostric M, Milger K, Krauss-Etschmann S, Engel M, Vestergaard G, Schloter M, et al. Development of a Stable Lung Microbiome in Healthy Neonatal Mice. Microb Ecol. 2018 Feb;75(2):529–42.

3. Wypych TP, Wickramasinghe LC, Marsland BJ. The influence of the microbiome on respiratory health. Nat Immunol. 2019 Oct;20(10):1279–90.

4. Biddle TA, Li Q, Maltz MR, Tandel PN, Chakraborty R, Yisrael K, et al. Salton Sea aerosol exposure in mice induces a pulmonary response distinct from allergic inflammation. Sci Total Environ. 2021 Oct;792:148450.

5. Biddle TA, Yisrael K, Drover R, Li Q, Maltz MR, Topacio TM, et al. Aerosolized aqueous dust extracts collected near a drying lake trigger acute neutrophilic pulmonary inflammation reminiscent of microbial innate immune ligands. Sci Total Environ. 2023 Feb;858:159882.

6. Dickson RP, Erb-Downward JR, Freeman CM, McCloskey L, Beck JM, Huffnagle GB, et al. Spatial Variation in the Healthy Human Lung Microbiome and the Adapted Island Model of Lung Biogeography. Ann Am Thorac Soc. 2015 Jun;12(6):821–30.

7. Lin L, Yi X, Liu H, Meng R, Li S, Liu X, et al. The airway microbiome mediates the interaction between environmental exposure and respiratory health in humans. Nat Med. 2023 Jul;29(7):1750–9.

8. Frie AL, Dingle JH, Ying SC, Bahreini R. The Effect of a Receding Saline Lake (The Salton Sea) on Airborne Particulate Matter Composition. Environ Sci Technol. 2017 Aug 1;51(15):8283–92.

9. Frie AL, Garrison AC, Schaefer MV, Bates SM, Botthoff J, Maltz M, et al. Dust Sources in the Salton Sea Basin: A Clear Case of an Anthropogenically Impacted Dust Budget. Environ Sci Technol. 2019 Aug 20;53(16):9378–88.

10. Jones BA, Fleck J. Shrinking lakes, air pollution, and human health: Evidence from California's Salton Sea. Sci Total Environ. 2020 Apr;712:136490.

11. Zucca C, Middleton N, Kang U, Liniger H. Shrinking water bodies as hotspots of sand and dust storms: The role of land degradation and sustainable soil and water management. CATENA. 2021 Dec;207:105669.

12. Farzan SF, Razafy M, Eckel SP, Olmedo L, Bejarano E, Johnston JE. Assessment of Respiratory Health Symptoms and Asthma in Children near a Drying Saline Lake. Int J Environ Res Public Health. 2019 Oct 11;16(20):3828.

13. Marshall J. Why Emergency Physicians Should Care About the Salton Sea. West J Emerg Med. 2017 Oct 18;18(6):1008–9.